論文 / 著書情報
Article / Book Information

Title	A conserved Ctp1/CtIP C-terminal peptide stimulates Mre11 endonuclease activity
Authors	Aleksandar Zdravković, James M. Daley, Arijit Dutta, Tatsuya Niwa, Yasuto Murayama, Shuji Kanamaru, Kentaro Ito, Takahisa Maki, Bilge Argunhan, Masayuki Takahashi, Hideo Tsubouchi, Patrick Sung, Hiroshi Iwasaki
Citation	Proceedings of the National Academy of Sciences of the United States of America, Vol. 118, No. 11, e2016287118
Pub. date	2021, 3
DOI	https://doi.org/10.1073/pnas.2016287118
Note	This file is author (final) version.

A Conserved Ctp1/CtIP C-Terminal Peptide Stimulates Mre11 Endonuclease Activity

Aleksandar Zdravković[1,2], James M. Daley[3], Arijit Dutta[3], Tatsuya Niwa[1,2], Yasuto Murayama[4], Shuji Kanamaru[1,2], Kentaro Ito[2], Takahisa Maki[2], Bilge Argunhan[2], Masayuki Takahashi[1], Hideo Tsubouchi[1,2]*, Patrick Sung[3]*, Hiroshi Iwasaki[1,2]*.

[1]School and Graduate School of Bioscience and Biotechnology, Tokyo Institute of Technology, 4259 Nagatsuta, Midori-ku, Yokohama, Kanagawa 226-8503, Japan.
[2]Institute of Innovative Research, Tokyo Institute of Technology, 4259 Nagatsuta, Midori-ku, Yokohama, Kanagawa 226-8503, Japan.
[3]Department of Biochemistry and Structural Biology, University of Texas Health Science Center, San Antonio, TX 78229, USA.
[4]Center for Frontier Research, National Institute of Genetics, 1111 Yata, Mishima, Shizuoka 411-8540, Japan.

*Correspondence to: htsubouchi@bio.titech.ac.jp, sungp@uthscsa.edu, hiwasaki@bio.titech.ac.jp

Classification
BIOLOGICAL SCIENCES

Keywords
Ctp1/CtIP, double-strand break repair, fission yeast, homologous recombination, Mre11-Rad50-Nbs1

Abstract

The Mre11-Rad50-Nbs1 complex (MRN) is important for repairing DNA double-strand breaks (DSBs) by homologous recombination (HR). The endonuclease activity of MRN is critical for resecting 5'-ended DNA strands at DSB ends, producing 3'-ended single-strand DNA, a prerequisite for HR. This endonuclease activity is stimulated by Ctp1, the *Schizosaccharomyces pombe* homolog of human CtIP. Here, with purified proteins, we show that Ctp1 phosphorylation stimulates MRN endonuclease activity by inducing the association of Ctp1 with Nbs1. The highly conserved extreme C-terminus of Ctp1 is indispensable for MRN activation. Importantly, a polypeptide composed of the conserved 15 amino acids at the C-terminus of Ctp1 (CT15) is sufficient to stimulate Mre11 endonuclease activity. Furthermore, the CT15 equivalent from CtIP can stimulate human MRE11 endonuclease activity, arguing for the generality of this stimulatory mechanism. Thus, we propose that Nbs1-mediated recruitment of CT15 plays a pivotal role in the activation of the Mre11 endonuclease by Ctp1/CtIP.

Significance statement

A DNA double-strand break (DSB) can be repaired accurately by homologous recombination (HR). The Mre11-Rad50-Nbs1 (MRN) complex is responsible for initiating homologous recombination by degrading 5’-ended DNA strand, where its activation by the Ctp1 cofactor plays a pivotal role. Here, by using purified fission yeast proteins, we show that two major elements comprise MRN activation. First, phosphorylation of Ctp1 promotes the physical interaction between MRN and Ctp1. Second, the C-terminus of Ctp1 activates nucleolytic processing of DSB ends. In the latter case, a small peptide comprising only 15 amino acids from the Ctp1 C-terminus is sufficient to activate MRN. Our results elucidate the core elements underlying MRN activation by Ctp1.

Main

Introduction

DNA double-strand breaks (DSBs) are potentially lethal lesions that threaten genomic integrity and cell viability. DSBs can occur spontaneously as a result of faulty DNA metabolism, or by exposure to genotoxins. In eukaryotes, these DSBs have ‘dirty ends’ that lack ligatable 3'-hydroxyl/5'-phosphate groups and are often firmly attached to proteins such as the Ku70-80 heterodimer and topoisomerases (1, 2). During meiosis, the topoisomerase-like Spo11 protein generates DSBs and remains covalently attached to the 5' DNA ends (3). To enable further processing, these DSB ends must be converted to ‘clean’ ends with 3'-hydroxyl/5'-phosphate groups properly exposed. This step is achieved by endonucleolytic cleavage, or clipping, by Mre11 (4–7).

In mammals, the MRE11, RAD50, and NBS1 complex (MRN), together with CtIP, is involved in the clipping reaction. MRE11 is the nuclease subunit that has both endonuclease and 3’-to-5’ exonuclease activities, but only the former is essential for clipping (4, 8–12). RAD50, a member of the Structural Maintenance of Chromosomes (SMC) protein family, binds to MRE11 to form an $(MRE11)_2$-$(RAD50)_2$ ring structure (MR complex) (13–15). NBS1 binds to the MR complex via MRE11 to form the MRN complex (16). Homologs of CtIP include Ctp1 in *Schizosaccharomyces pombe* and Sae2 in *Saccharomyces cerevisiae* (17–19). Upon phosphorylation, these proteins physically interact with their cognate MRN complex via the N-terminal forkhead-associated domain of NBS1, leading to activation of the MRE11 endonucleolytic clipping activity (20–24). However, the mechanistic details underlying this activation have not yet been determined.

Through biochemical reconstitution using fission yeast proteins, we made three key findings regarding how Ctp1 activates MRN. First, MRN activation is mediated by Ctp1 phosphorylation, which promotes the direct association of Ctp1 with the Nbs1 subunit of MRN. Second, the highly conserved extreme C-terminus of Ctp1 retains the ability to promote the endonuclease activity of MRN. Strikingly, a synthetic polypeptide comprising the 15 amino acids from the extreme C-terminus of Ctp1 was sufficient for the full activation of MRN. Third, we verified the evolutionary significance of these findings by demonstrating that the conserved C-terminal polypeptide of CtIP can also stimulate the endonuclease activity of human MRN. Together, our results strongly suggest that the Ctp1-promoted MRN activation mechanism consists of at least two, fundamentally separable elements: phosphorylation-induced Ctp1-MRN association and activation of MRN by the C-terminal peptide of Ctp1. Thus, recruitment of the Ctp1 C-terminus to MRN is likely pivotal to this

activation mechanism.

Results

Phosphorylation of Ctp1 by Casein Kinase II Promotes the Physical Interaction Between MRN and Ctp1

To analyze the interaction between MRN and Ctp1, we purified the *S. pombe* MR complex, Nbs1 and Ctp1 (SI Appendix, Fig. S1A). Previous studies suggested that casein kinase II (CK2) phosphorylates residues in the SXT domain of Ctp1 (Ser-77, Thr-78, Thr-79, Ser-87, and Thr-89) (17, 21, 25). Thus, the catalytic subunit of the *S. pombe* CK2 ortholog Cka1 was purified (SI Appendix, Fig. S1B) and incubated with Ctp1 in the presence of ATP. Upon Cka1 treatment, a mobility shift of Ctp1 was observed by sodium dodecyl sulfate polyacrylamide-gel electrophoresis (SDS-PAGE; Fig. 1A). This shift was abolished upon λ-phosphatase treatment, suggesting that it was caused by phosphorylation of Ctp1. Notably, in a variant of Ctp1 where the five phosphorylatable residues of the SXT domain were all substituted to alanine (SXT-5A), the extent of the shift was greatly reduced, although a subtle mobility shift still remained (Fig. 1A). Further analysis of phosphorylated Ctp1 by mass spectrometry revealed additional phosphorylated residues besides those in the SXT domain (Ser-151, Thr-154 and Thr-155; Fig. 1B, SI Appendix, Table S1).

The forkhead-associated domain situated in the N-terminal region of Nbs1 has been shown to bind several phosphopeptides derived from the Ctp1 SXT site with micromolar order affinity (21). Pull-down experiments with FLAG-tagged Nbs1 demonstrated that full-length Ctp1 was pulled down by Nbs1 in a phosphorylation-dependent manner (Fig. 1C). Cka1-treated SXT-5A was not pulled down, whereas an N-terminal 120 amino-acid fragment of Ctp1 (1-120) that lacked all the phosphorylation residues except those within the SXT domain was pulled down by Nbs1-FLAG, demonstrating that Ctp1 binds to Nbs1 via the phosphorylated SXT site.

Ctp1 is known to form a tetramer (26). Thus, we asked if phosphorylation affects its oligomerization. Size-exclusion chromatography with multiangle light scattering (SEC-MALS) was employed to determine the molecular weight of Ctp1 variants. Similar to unphosphorylated wild-type Ctp1, the molecular weight of phosphorylated Ctp1 corresponded well to that of a tetramer (Fig. 1D, top). Similarly, the molecular weight of Ctp1(SXT-5A) also corresponded well to that of a tetramer without any appearance of extra SEC peaks which might indicate altered oligomeric status (Fig. 1D, bottom), arguing that 5 mutations within the SXT domain do not alter its oligomerization.

We next reconstituted the higher-order complex of MRN-Ctp1 (Fig. 1E). In the presence of Rad50 and Nbs1, hexahistidine-tagged Mre11 (Mre11-6×H) pulled down

phosphorylated Ctp1, but not unphosphorylated Ctp1. Notably, Mre11-6×H did not pull down phosphorylated Ctp1 in the absence of Nbs1, indicating that incorporation of phosphorylated Ctp1 into the higher-order complex requires Nbs1.

Ctp1 Activates the Endonuclease Activity of MRN Through Interaction with Nbs1

To test the endonucleolytic activity of the MRN-Ctp1 complex, we employed a fluorescently-labeled 70 bp DNA duplex with biotin-streptavidin bound to the ends of each strand (Fig. 2A) (27). Addition of phosphorylated Ctp1 (100 nM monomers) to the reaction containing an equimolar amount of MRN subunits and dsDNA ends caused active cleavage of the streptavidin-bound substrate, whereas very little cleavage was seen with MRN alone (Fig. 2B). In the absence of MRN, Ctp1 did not display any endonuclease activity. The MRN complex containing a nuclease-deficient Mre11 (H134S; ND in Fig. 2B) did not yield any cleavage products, even in the presence of phosphorylated Ctp1, indicating that the endonucleolytic cut was performed by the Mre11 active site. Similar to previous reports with human and *S. cerevisiae* proteins (9, 28), both Mn^{2+} and Mg^{2+} are required for phosphorylated Ctp1-dependent stimulation of MRN (SI Appendix, Fig. S2A). ATP stimulated the phosphorylated Ctp1-dependent endonuclease of MRN, but ADP, AMP-PNP and ATPγS did not (SI Appendix, Fig. S2B), suggesting that ATP hydrolysis by the ABC-type ATPase of Rad50 is required for this stimulation (9, 11, 29, 30).

Notably, unphosphorylated Ctp1 stimulated the endonuclease activity of Mre11, albeit to a lesser extent than phosphorylated Ctp1 (Fig. 2B). Titration experiments (Fig. 2C, SI Appendix, Fig. S3) demonstrated that near-maximal levels of DNA cleavage were achieved at an equimolar concentration to MRN (100 nM) with phosphorylated Ctp1, while unphosphorylated Ctp1 did not fully stimulate the endonuclease activity, even at a 30 times higher concentration. These results suggest that the phosphorylation of Ctp1, most likely at the SXT site, stimulates MRN endonuclease activity through enhanced interaction of Ctp1 with MRN. Unlike the endonuclease activity, neither the exonuclease nor the ATPase activity of MRN was stimulated by phosphorylated Ctp1 (SI Appendix, Fig. S4).

Because higher-order MRN-Ctp1 complex formation requires Nbs1, we assessed the influence of Nbs1 on endonuclease stimulation (Fig. 2C, SI Appendix, Fig. S3). In the absence of Nbs1, the stimulation conferred by Ctp1 was independent of phosphorylation and comparable in magnitude to that seen with unphosphorylated Ctp1 in the presence of Nbs1. Ctp1(SXT-5A) also stimulated MR endonuclease to a similar level as unphosphorylated Ctp1 (SI Appendix, Fig. S5A). These results argue that Nbs1 is only required for the endonuclease stimulation by phosphorylated Ctp1, while also raising the possibility that a region(s) other than the phosphorylated SXT domain might contribute to

this activity.

The C-Terminus of Ctp1 Is Critical for Stimulating the Endonuclease Activity of MRN

In order to examine the relationship between Ctp1 oligomerization and MR endonuclease activation, two mutant proteins that affect oligomer formation differently were employed. Ctp1(15-294) forms dimers whereas Ctp1(189-294) exists as monomer (SI Appendix, Fig. S5B). In both cases, stimulation of MR was comparable to that by unphosphorylated Ctp1, indicating tetramerization per se is not essential for MR activation. Strikingly, while the N-terminal truncation (i.e., Ctp1(189-294)) stimulated MR endonuclease activity similarly to the full-length Ctp1, the C-terminal truncation (residues 1-250) had little stimulatory effect (Fig. 2D). This strongly argues that the C-terminal region of Ctp1, from residue 189 onwards and lacking the SXT domain, has a role in the activation of the MR endonuclease that is independent of Nbs1 (17, 18, 31, 32).

Next, the CxxC and RHR motifs commonly found in the C-terminal region of CtIP-family proteins (17, 18) were investigated by mutating CxxC to SxxS or RHR to RAA. These mutant proteins still stimulated MRN endonuclease activity, but at a lower level than wild-type Ctp1 (Fig. 2E), indicating that these two motifs in the C-terminal region are relevant to, but not essential for, endonuclease stimulation.

Next, we turned our attention to a C-terminal 15-amino-acid sequence (CT15 hereafter), which is relatively conserved in eukaryotes (Fig. 3A). We assessed the importance of this sequence by a multicopy-plasmid-based complementation test using the *ctp1*Δ mutant and DNA damage sensitivity to camptothecin (CPT). CPT inhibits topoisomerase I, resulting in the accumulation of reaction intermediates with topoisomerase I covalently attached to DNA ends, which require MRN to be removed (2, 33). Overexpression of two full-length Ctp1 variants with multiple conserved residues replaced with alanine—CT15-5A (P284A, F287A, W288A, E289A, F292A) and FWE-3A (F287A, W288A, E289A)—were unable to complement the DNA damage sensitivity of the *ctp1*Δ strain (Fig. 3B). Furthermore, *ctp1*Δ cells expressing Ctp1 variants with a single-residue substitution—F287A, W288A or F292A—showed a severe defect in DNA repair (Fig. 3B). Strains with the corresponding mutations at the native chromosomal locus also showed similar DNA damage sensitivity (Fig. 3C).

Sporulation requires the removal of covalently attached Rec12 (Spo11) from DSB ends by the MRN endonuclease (31, 34). The viable spore yield of strains containing short Ctp1 truncations (Ctp1 residues 1-279, 1-286) was as severely reduced as the *ctp1*Δ mutant (Fig. 3D). Mutations at the three critical amino acids identified above (F287A, W288A or F292A; Fig. 3B) also showed a substantial reduction in viable spore yield.

We then directly compared C-terminal mutants with those where CxxC or RHR are mutated (i.e., C226S, C229S and H274A, R275A, respectively). *ctp1*Δ cells overexpressing these Ctp1 variants showed similar CPT sensitivity to two CT15 mutants, FWE-3A and W288A, which themselves resemble the null mutant (SI Appendix, Fig. S6A). Strains carrying these mutations at the *ctp1*$^{+}$ locus also showed severe CPT sensitivity comparable to the null mutant, except that, at 0.5 μM CPT, the H274A, R275A mutant showed slightly milder sensitivity than other mutants (SI Appendix, Fig. S6B). The levels of DNA damage sensitivity seen in the CxxC and RHR motif mutants are essentially in line with those reported previously (18, 26, 31). This observation, together with the data showing that purified CxxC and RHR-mutated proteins still retain the ability to stimulate MR endonuclease activity, suggest the involvement of CxxC and RHR motifs in enhancing the effect of CT15.

Collectively, these results support the idea that CT15 and its three conserved amino acids are critical for the role of MRN in the repair of DNA damage during vegetative growth and the removal of DSB-associated Rec12 during sporulation.

Conserved 15 Amino-Acid Peptide from the C-Terminus of Ctp1 Is Sufficient for Stimulating the Endonuclease Activity of MRN

Our results suggested that CT15 might be the functional element responsible for the stimulation of MR endonuclease activity. We therefore introduced a synthetic CT15 peptide into an endonuclease assay containing the MR complex, but lacking Nbs1 (Fig. 4A). Strikingly, the CT15 peptide stimulated the endonuclease activity of MR similarly to the unphosphorylated, full-length Ctp1 (Fig. 4B). Moreover, stimulation of MR at higher concentrations of the CT15 peptide (100 μM) was comparable to the maximal levels achieved with the MRN complex and phosphorylated full-length Ctp1 (Ctp1p in Fig. 4C). Importantly, CT15 stimulated both MRN and MR to a similar level (compare Fig. 4B and Fig. 4C), suggesting that a high dose of CT15 bypassed the requirement for the Nbs1-mediated phosphorylation-dependent Ctp1 recruitment mechanism. CT15 synthetic peptide variants, each with one of the three critical aromatic residues replaced by alanine (F287A, W288A, or F292A), were severely defective in MR stimulation (Fig. 4D). As synthetic CT15 itself has no endonuclease activity (Figs. 4B-D), these results strongly suggest that the CT15 peptide itself is practically sufficient to function as an activator for the MR endonuclease.

We considered the possibility that the function of CT15 might be evolutionally conserved. Interestingly, alignment of CT15 sites revealed that T847 and T859 in human CtIP, which are phosphorylated by CDK and ATM, respectively, are located within or one amino acid outside of the aligned site (Fig. 3A). Mutation of these residues to alanine has

been shown to severely compromise the ability of CtIP to stimulate MRN (22, 23, 35, 36); we therefore speculated that they might directly regulate the CT15 peptide. The CT15 site in human CtIP was extended to a total of 19 amino acids to encompass both phosphorylation sites (human CT15 extended, hCT15e), and several peptides were synthesized (wild type and mutant variants).

Remarkably, we found that the hCT15e peptide with both T847 and T859 phosphorylated stimulated the endonuclease activity of human MRN (hMRN; Fig. 4E). By contrast, weak stimulation of hMRN was observed for hCT15e with only T847 phosphorylated, while stimulation was barely seen when unphosphorylated peptide, or a peptide only phosphorylated at T859, were employed. Importantly, alanine substitution of conserved residues corresponding to F851 and W852 resulted in a loss of stimulation even when both T847 and T859 were phosphorylated. These results demonstrate that the hCT15e peptide also retains the capacity to stimulate human MRN endonuclease activity, but only when conserved CDK and ATM target sites are phosphorylated.

Discussion

Through biochemical reconstitution, we demonstrate that phosphorylation of Ctp1 within the SXT domain by casein-kinase II promotes robust binding of Ctp1 to Nbs1, stimulating the endonuclease activity of MRN. What is central to this stimulation mechanism is the extreme C-terminus of Ctp1 designated as CT15, which only contains 15 amino acids and can fully stimulate the endonuclease activity of MR. Furthermore, the human counterpart of CT15 can also stimulate human MRN as long as two associated residues, T847 and T859, are phosphorylated. We propose that the core of MRN endonuclease stimulation is provided by CT15 whose effectiveness is promoted by the phosphorylation-dependent recruitment of Ctp1 to MRN.

Our current understanding of the role of Ctp1/Sae2/CtIP in DNA end resection primarily stems from the in vivo and in vitro analysis of loss of function mutants. In this paper, we take a synthetic approach and demonstrate that the MR complex is stimulated by the CT15 peptide. This observation narrows down the MR activation domain from the loosely defined C-terminus to this particularly small peptide element, shedding light on the interpretation of previously described Ctp1 mutants. The peak of MR activity stimulated by the CT15 peptide was comparable to that of MRN stimulated by CK2-phosphorylated Ctp1. However, while phosphorylated Ctp1 could achieve this level of stimulation at approximately stoichiometric concentrations, a vast excess of CT15 was required to potentiate MR to a similar degree. Based on this, we posit that the phosphorylation-dependent recruitment of

Ctp1 to MRN upregulates the activity of the CT15 peptide by 100-1000–fold. A flexible intrinsically disordered region within Ctp1 connects the CT15 site in the extreme C-terminus to the N-terminally located SXT domain. Phosphorylation of the SXT domain promotes its binding to the N-terminal FHA domain of Nbs1. The FHA domain of Nbs1 is connected to the C-terminally located Mre11 interacting domain via a flexible loop. Taken together, these topological observations suggest that the CT15 site is flexibly tethered by Nbs1 at the phosphorylated SXT domain, thus accessible to the area within a radius of approximately 300 Å from the Mre11 dimer-dimer interface (21, 26). Sequestering CT15 in close proximity to MR is expected to result in a local concentration increase that likely compensates for the suboptimal activity of CT15. The 300 Å tethering range would allow CT15 to potentially interact with any part of Mre11 including the catalytic site, the head domain of Rad50 and even part of the coiled-coil regions as well as any bound DNA.

We are considering the possibility that CT15 binding to MR induces/stabilizes a critical conformational change leading to efficient cleavage of end-blocked DNA. Recently, the structural homolog of the MR complex from bacteria, SbcCD, was shown to adopt a drastic conformational change (“cutting state”) upon sensing a DNA break (13). SbcCD also exhibits endonuclease activity on DNA end-blocked substrates, but unlike MR, this activity appears to be inherent to SbcCD since neither Nbs1 nor Ctp1 has been identified in prokaryotes. A structural element named the fastener loop of SbcD (Mre11) interacts with the outer β-sheet of SbcC (Rad50) in the cutting state of the complex, and this binding surface corresponds to the cluster of Rad50S mutations within *S. cerevisiae*. Additionally, interaction of the phosphorylated C-terminus of Sae2 with Rad50 is abolished upon introduction of a *RAD50S* mutation (K81I) found in the same cluster (37). These observations raise the possibility that CT15 might promote the association of Mre11 and Rad50 through the fastener loop interface, possibly even bridging the interaction between Rad50 and Mre11, which would work in favor of forming/maintaining the cutting state conformation of the MR complex similar to SbcCD (38, 39).

It is also possible that CT15 promotes MR endonuclease through DNA binding. The core FWE motif within the CT15 site conforms to the mismatch recognition FxE motif found within MSH6 of the MutSα complex (40, 41). The “x” in the FxE motif is usually an aromatic residue, with human MSH6 harboring FYE and *S. cerevisiae* Msh6 containing FFE. However, unlike the FWE motif, the conserved FxE motif is located within a β-strand situated in a structurally well-defined environment of MutS where it contacts a mispaired base (with support from multiple other residues). If there is any functional similarity within the FXE motifs of Ctp1/CtIP and MSH6, it is likely achieved in conjunction with structural support from another well-structured protein like Mre11 or Rad50.

Ctp1 and its human homolog CtIP form a tetramer (26, 42). Mutations that impair tetramer formation in CtIP (9) and Sae2 (37) did not fully abolish its capacity to activate MR; a residual stimulation was still seen in both cases. Similarly, in our assay, stimulation of MR by Ctp1 was seen regardless of its oligomeric status, indicating tetramerization per se is not essential for MR activation (SI Appendix, Fig. S5B). This, however, does not exclude the involvement of tetramerization in MR activation; impairment of tetramerization leads to a great reduction in MR activation and DNA repair deficiency after all (26, 43). It is reasonable, for example, to assume that the recruitment of a tetramer containing four CT15 activators, mediated through the interaction between Nbs1 and phosphorylated Ctp1, would stimulate MR more than the recruitment of a single Ctp1 molecule by elevating the local concentration of CT15. Tetramerization of Ctp1 is necessary for bridging DNA molecules in the absence of MRN (26, 43). Thus, it is also possible that some form of DNA bridging acts in favor of enhancing the overall efficiency of MR activation.

The CT15 equivalent in CtIP, which we identified based on sequence homology to *S. pombe* CT15, is highly conserved within higher eukaryotes. Interestingly, two of the critically important phosphorylation sites in human CtIP, T847 and T859, are located within and adjacent to the CT15 site, which prompted us to expand the CT15 site to include them—generating the hCT15e peptide—and test the phosphorylated versions of this peptide. Notably, mutations of these residues to alanine have been shown to severely impact the effect of CtIP related to MRN endonuclease activity both in vivo and in vitro (22, 35, 36, 44). Here, we show that phosphorylation of T847 and T859 together serve the role to reconstitute the active form of the CT15 cofactor necessary for the stimulation of hMRN endonuclease activity. The peptide, when doubly phosphorylated, showed the most robust MRN stimulation. Mutation of the critical aromatic residues within the CT15 site resulted in a loss of stimulation even in the double-phosphorylated peptide, suggesting that the phosphorylation of these sites directly regulates the activity of CT15 in CtIP.

Defining the novel CT15 site in the Ctp1/Sae2/CtIP ortholog family shifts the focus from the already recognized CXXC and RHR motifs and clearly defines the critical site for MRN activation. This is important for our interpretation of the previously reported mutant phenotypes. It is likely that the Seckel and Jawad syndromes are in fact at least in part caused by the loss of CT15 functionality as both reported truncations lack this site (45). Furthermore, reducing the size of an MRN activator to that of a peptide opens the possibility of practical uses. Modification of the CT15 peptide could yield a stronger activator or a potential inhibitor of the MRN complex. Activation or inhibition of the MRN complex could be particularly useful in gene editing downstream from CRISPR-Cas9 or other targeted nucleases as it could shift the bias between non-homologous end joining and homologous

recombination repair. Alternatively, CT15-derived peptides could prove to be useful as cancer therapeutics or radiotherapy sensitizers (46, 47).

Materials and Methods

Endonuclease assay

Standard endonuclease assays were performed in 4 µl of reaction mixture containing 150 mM NaCl, 20 mM Tris-HCl [pH 7.5], 10% glycerol, 1 mM DTT, 0.5 mM $MnCl_2$, 5 mM $MgCl_2$, 50 nM DNA , 2 mM ATP, 1 µM streptavidin, 50 nM dsDNA, 50 nM $(Mre11)_2(Rad50)_2$, 100 nM Nbs1, and the indicated amounts of Ctp1. Reactions were incubated for 1 h at 30°C and then stopped by addition of 1 µl stop reagent (1:1:1 mixture of proteinase K [Takara], 0.5 M EDTA [pH 8.0] and 10% SDS) and by incubation at 50°C for 20 min. Four volumes of formamide loading buffer (20 mM EDTA, 0.05 mg/ml Orange G, and 96% formamide) were added to the samples, which were incubated at 98°C for 7 min and then loaded on 13.3% polyacrylamide gels containing 8 M urea. DNA substrate and products attached to TAMRA were visualized with a Typhoon FLA 9500 imager (GE Healthcare). Band quantification was performed with ImageQuant TL v8.1.0.0 (GE Healthcare). Briefly, for each lane, total and uncut DNA band signals were quantified; background based on unoccupied corresponding areas of the gel was subtracted; and the amount of degraded DNA was expressed as the percentage of the total lane signal, based on the initial uncut-band signal.

Data Availability

All relevant data are presented in the manuscript. Requests for reagents or further information should be directed to H.T. (htsubouchi@bio.titech.ac.jp), P.S. (sungp@uthscsa.edu) or H.I. (hiwasaki@bio.titech.ac.jp).

Additional Materials and Methods are in the *SI Appendix*.

Acknowledgments: We thank Yumiko Kurokawa for help with protein purification. We are grateful to members of the Iwasaki laboratory for discussion and encouragement.

Funding: This study was supported in part by the Japan Society for the Promotion of Science, Grants-in-Aid for Scientific Research on Innovative Areas (15H059749 to H.I.), for Scientific Research (A) (18H03985 to H.I.), for Young Scientists (B) (17K15061 to B.A.), for Scientific Research (B) (18H02371 to H.T. and 19H03160 to Y.M.), for Early-Career Scientists (19K16039 to K.I. and 20K15713 to B.A.) and by US National Institutes of Health grant R35 CA241801 (to P.S.).

Competing interests: The authors declare no competing interests.

Author contributions: A.Z., P.S., and H.I. conceived and designed the study. J.M.D. and A.D. purified the human MRN complex. K.I. and T.M. helped with all other protein purifications. T.N. performed MS experiments. A.Z. performed all other experiments. A.Z. and T.N. analyzed MS data. A.Z., J.M.D., A.D., Y.M., S.K., K.I., T.M., B.A., M.T., H.T., P.S., and H.I. analyzed all other data. Y.M., S.K., K.I., T.M., B.A., M.T., H.T., P.S., and H.I. provided expertise and reagents. Y.M., S.K., M.T., H.T., P.S., and H.I. supervised the study. A.Z., T.N., Y.M., B.A., H.T., P.S., and H.I. contributed to writing the manuscript.

References

1. D. Wu, L. M. Topper, T. E. Wilson, Recruitment and Dissociation of Nonhomologous End Joining Proteins at a DNA Double-Strand Break in *Saccharomyces cerevisiae*. *Genetics* **178**, 1237–1249 (2008).
2. E. Hartsuiker, M. J. Neale, A. M. Carr, Distinct Requirements for the Rad32^{Mre11} Nuclease and Ctp1^{CtIP} in the Removal of Covalently Bound Topoisomerase I and II from DNA. *Mol. Cell* **33**, 117–123 (2009).
3. S. Keeney, C. N. Giroux, N. Kleckner, Meiosis-specific DNA double-strand breaks are catalyzed by Spo11, a member of a widely conserved protein family. *Cell* **88**, 375–384 (1997).
4. A. Shibata, *et al.*, DNA Double-Strand Break Repair Pathway Choice Is Directed by Distinct MRE11 Nuclease Activities. *Mol. Cell* **53**, 7–18 (2014).
5. Z. Zhu, W.-H. H. Chung, E. Y. Shim, S. E. Lee, G. Ira, Sgs1 Helicase and Two Nucleases Dna2 and Exo1 Resect DNA Double-Strand Break Ends. *Cell* **134**, 981–994 (2008).
6. V. Garcia, S. E. L. Phelps, S. Gray, M. J. Neale, Bidirectional resection of DNA double-strand breaks by Mre11 and Exo1. *Nature* **479**, 241–244 (2011).
7. P. Langerak, E. Mejia-Ramirez, O. Limbo, P. Russell, Release of Ku and MRN from DNA Ends by Mre11 Nuclease Activity and Ctp1 Is Required for Homologous Recombination Repair of Double-Strand Breaks. *PLoS Genet.* **7**, e1002271 (2011).
8. A. Syed, J. A. Tainer, The MRE11–RAD50–NBS1 Complex Conducts the Orchestration of Damage Signaling and Outcomes to Stress in DNA Replication and Repair. *Annu. Rev. Biochem.* **87**, 263–294 (2018).
9. R. Anand, L. Ranjha, E. Cannavo, P. Cejka, Phosphorylated CtIP Functions as a Co-factor of the MRE11-RAD50-NBS1 Endonuclease in DNA End Resection. *Mol. Cell* **64**, 940–950 (2016).
10. R. A. Deshpande, J. H. Lee, S. Arora, T. T. Paull, Nbs1 Converts the Human Mre11/Rad50 Nuclease Complex into an Endo/Exonuclease Machine Specific for Protein-DNA Adducts. *Mol. Cell* **64**, 593–606 (2016).
11. W. Wang, J. M. Daley, Y. Kwon, D. S. Krasner, P. Sung, Plasticity of the Mre11–Rad50–Xrs2–Sae2 nuclease ensemble in the processing of DNA-bound obstacles. *Genes Dev.* **31**, 2331–2336 (2017).
12. G. Reginato, E. Cannavo, P. Cejka, Physiological protein blocks direct the Mre11-Rad50-Xrs2 and Sae2 nuclease complex to initiate DNA end resection. *Genes Dev.* **31**, 2325–2330 (2017).
13. L. Käshammer, *et al.*, Mechanism of DNA End Sensing and Processing by the

Mre11-Rad50 Complex. *Mol. Cell* **76**, 382-394.e6 (2019).

14. H. Tatebe, *et al.*, Rad50 zinc hook functions as a constitutive dimerization module interchangeable with SMC hinge. *Nat. Commun.* **11**, 370 (2020).
15. Y. Liu, *et al.*, ATP-dependent DNA binding, unwinding, and resection by the Mre11/Rad50 complex. *EMBO J.* **35**, 743–58 (2016).
16. C. B. Schiller, *et al.*, Structure of Mre11–Nbs1 complex yields insights into ataxia-telangiectasia–like disease mutations and DNA damage signaling. *Nat. Struct. Mol. Biol.* **19**, 693–700 (2012).
17. Y. Akamatsu, *et al.*, Molecular Characterization of the Role of the *Schizosaccharomyces pombe nip1+/ctp1+* Gene in DNA Double-Strand Break Repair in Association with the Mre11-Rad50-Nbs1 Complex. *Mol. Cell. Biol.* **28**, 3639–3651 (2008).
18. O. Limbo, *et al.*, Ctp1 is a cell-cycle-regulated protein that functions with Mre11 complex to control double-strand break repair by homologous recombination. *Mol. Cell* **28**, 134–46 (2007).
19. A. H. Z. McKee, N. Kleckner, A general method for identifying recessive diploid-specific mutations in *Saccharomyces cerevisiae*, its application to the isolation of mutants blocked at intermediate stages of meiotic prophase and characterization of a new gene *SAE2*. *Genetics* **146**, 797–816 (1997).
20. A. A. Sartori, *et al.*, Human CtIP promotes DNA end resection. *Nature* **450**, 509–514 (2007).
21. R. S. Williams, *et al.*, Nbs1 Flexibly Tethers Ctp1 and Mre11-Rad50 to Coordinate DNA Double-Strand Break Processing and Repair. *Cell* **139**, 87–99 (2009).
22. H. Wang, *et al.*, The Interaction of CtIP and Nbs1 Connects CDK and ATM to Regulate HR–Mediated Double-Strand Break Repair. *PLoS Genet.* **9**, e1003277 (2013).
23. R. Anand, *et al.*, NBS1 promotes the endonuclease activity of the MRE11- RAD50 complex by sensing CtIP phosphorylation. *EMBO J.* **38**, 1–16 (2019).
24. E. Cannavo, G. Reginato, P. Cejka, Stepwise 5′ DNA end-specific resection of DNA breaks by the Mre11-Rad50-Xrs2 and Sae2 nuclease ensemble. *Proc. Natl. Acad. Sci. U. S. A.* **116**, 5505–5513 (2019).
25. G. E. Dodson, O. Limbo, D. Nieto, P. Russell, Phosphorylation-regulated binding of Ctp1 to Nbs1 is critical for repair of DNA double-strand breaks. *Cell Cycle* **9**, 1516–1522 (2010).
26. S. N. Andres, *et al.*, Tetrameric Ctp1 coordinates DNA binding and DNA bridging in DNA double-strand-break repair. *Nat. Struct. Mol. Biol.* **22**, 158–166 (2015).
27. R. Anand, C. Pinto, P. Cejka, Methods to Study DNA End Resection I: Recombinant Protein Purification. *Methods Enzymol.* **600**, 25–66 (2018).

28. E. Cannavo, P. Cejka, Sae2 promotes dsDNA endonuclease activity within Mre11-Rad50-Xrs2 to resect DNA breaks. *Nature* **514**, 122–125 (2014).
29. R. A. Deshpande, J.-H. Lee, T. T. Paull, Rad50 ATPase activity is regulated by DNA ends and requires coordination of both active sites. *Nucleic Acids Res.* **45**, 5255–5268 (2017).
30. H. B. D. Prasada Rao, *et al.*, A SUMO-ubiquitin relay recruits proteasomes to chromosome axes to regulate meiotic recombination. *Science (80-.).* **355** (2017).
31. L. Ma, N. Milman, M. Nambiar, G. R. Smith, Two separable functions of Ctp1 in the early steps of meiotic DNA double-strand break repair. *Nucleic Acids Res.* **43**, 7349–7359 (2015).
32. K. L. Jensen, P. Russell, Ctp1-dependent clipping and resection of DNA double-strand breaks by Mre11 endonuclease complex are not genetically separable. *Nucleic Acids Res.* **44**, 8241–8249 (2016).
33. Y. Pommier, *et al.*, Repair of Topoisomerase I-Mediated DNA Damage. *Prog. Nucleic Acid Res. Mol. Biol.* **81**, 179–229 (2006).
34. E. Hartsuiker, *et al.*, Ctp1CtIP and Rad32^{Mre11} Nuclease Activity Are Required for Rec12^{Spo11} Removal, but Rec12^{Spo11} Removal Is Dispensable for Other MRN-Dependent Meiotic Functions. *Mol. Cell. Biol.* **29**, 1671–1681 (2009).
35. P. Huertas, S. P. Jackson, Human CtIP Mediates Cell Cycle Control of DNA End Resection and Double Strand Break Repair. *J. Biol. Chem.* **284**, 9558–9565 (2009).
36. R. A. Deshpande, *et al.*, DNA-dependent protein kinase promotes DNA end processing by MRN and CtIP. *Sci. Adv.* **6**, eaay0922 (2020).
37. E. Cannavo, *et al.*, Regulatory control of DNA end resection by Sae2 phosphorylation. *Nat. Commun.* **9**, 1–14 (2018).
38. J. C. Connelly, E. S. De Leau, D. R. F. Leach, Nucleolytic processing of a protein-bound DNA end by the E. coli SbcCD (MR) complex. *DNA Repair (Amst).* **2**, 795–807 (2003).
39. J. H. Saathoff, L. Käshammer, K. Lammens, R. T. Byrne, K. P. Hopfner, The bacterial Mre11–Rad50 homolog SbcCD cleaves opposing strands of DNA by two chemically distinct nuclease reactions. *Nucleic Acids Res.* **46**, 11303–11314 (2018).
40. N. Kato, *et al.*, Sensing and Processing of DNA Interstrand Crosslinks by the Mismatch Repair Pathway. *Cell Rep.* **21**, 1375–1385 (2017).
41. J. J. Warren, *et al.*, Structure of the Human MutSα DNA Lesion Recognition Complex. *Mol. Cell* **26**, 579–592 (2007).
42. O. R. Davies, *et al.*, CtIP tetramer assembly is required for DNA-end resection and repair. *Nat. Struct. Mol. Biol.* **22**, 150–157 (2015).
43. S. N. Andres, Z. M. Li, D. A. Erie, R. S. Williams, Ctp1 protein–DNA filaments promote DNA bridging and DNA double-strand break repair. *J. Biol. Chem.* **294**, 3312–3320

(2019).

44. P. Huertas, F. Cortés-Ledesma, A. A. Sartori, A. Aguilera, S. P. Jackson, CDK targets Sae2 to control DNA-end resection and homologous recombination. *Nature* **455**, 689–692 (2008).

45. P. Qvist, *et al.*, CtIP mutations cause Seckel and Jawad syndromes. *PLoS Genet.* **7** (2011).

46. A. Dupré, *et al.*, A forward chemical genetic screen reveals an inhibitor of the Mre11-Rad50-Nbs1 complex. *Nat. Chem. Biol.* **4**, 119–125 (2008).

47. C. V. Kavitha, B. Choudhary, S. C. Raghavan, K. Muniyappa, Differential regulation of MRN (Mre11-Rad50-Nbs1) complex subunits and telomerase activity in cancer cells. *Biochem. Biophys. Res. Commun.* **399**, 575–580 (2010).

Figure Legends

Fig. 1. Phosphorylation of the SXT site of Ctp1 by Cka1 recruits Ctp1 to the MRN complex. (A) *In vitro* phosphorylation of Ctp1 variants by the CK2 catalytic subunit Cka1. (B) Summary of phosphorylation sites of Ctp1, revealed by mass spectrometry. (C) Interaction of Ctp1 variants and Nbs1, examined by co-immunoprecipitation with Nbs1-FLAG. (D) Molecular masses of phosphorylated Ctp1 and SXT-5A mutant were evaluated by SEC-MALS. Estimated molecular mass: Ctp1(unmodified) = 142.0 kDa, Phosphorylated Ctp1 = 138.5 kDa, SXT-5A = 141.6 kDa. Theoretical molecular mass of unmodified Ctp1 monomer is 33.1 kDa. (E) MRN-Ctp1 complex formation and its requirement, examined by co-immunoprecipitation with hexahistidine-tagged Mre11 (Mre11-6xH).

Fig. 2. Stimulation of Mre11 endonuclease activity by Ctp1 is enhanced by Cka1 phosphorylation in the presence of Nbs1. (A) Substrate used for assaying Mre11 endonuclease activity. (B) MRN endonuclease activity was assayed with phosphorylated (red “p”) or unphosphorylated Ctp1. ND, an MRN complex containing nuclease-deficient $Mre11^{H134S}$. (C) Titration of unphosphorylated Ctp1 (Ctp1) and phosphorylated Ctp1 (Ctp1p) in the endonuclease assay. Error bars, SD; *n* = 3. n/d, not determined. A representative gel image is shown in SI Appendix, Fig. S3. (D) Mre11 endonuclease activity in assays involving the Mre11-Rad50 complex and full-length or truncated Ctp1. (E) The effect of substitutions in the CxxC and RHR motifs on MRN endonuclease stimulation. Ctp1 (WT, truncated or mutant proteins) is at 3 μM in (D) and (E).

Fig. 3. The ability of Ctp1 to promote Mre11 activity in vivo is located within a conserved 15 amino-acid sequence at the C-terminus (CT15). (A) Sequence alignment of CtIP/Ctp1 C-terminus. Thr-847 and Thr-859 in human CtIP are phosphorylation sites for CDK and ATM, respectively. (B) Complementation of *ctp1Δ* camptothecin sensitivity with plasmids expressing Ctp1 variants. (C) Camptothecin sensitivity of strains with mutations in CT15 at the endogenous *ctp1* locus. Serially diluted cells were spotted onto YES plates containing camptothecin. (D) Relative viable spore yield of various *ctp1* mutants. Error bars, SD; n = 3.

Fig. 4. A conserved 15 amino-acid peptide (CT15) is sufficient to stimulate MRN endonuclease activity (A) Location of CT15 in reference to the full length Ctp1. (B) Endonuclease activity of MR was assayed in the presence of CT15 peptides. (C) Same as

(B) except that MRN was used. (D) Same as (B) but CT15 variants mutated at conserved amino acids were used at 100 μM. (E) A synthetic peptide of the human CT15 counterpart (hCT15e) stimulates hMRN endonuclease activity when its CDK and ATM target sites (Thr-847 and Thr-859, respectively) are phosphorylated. In this assay, hMRN was introduced at 100 nM with respect to the concentration of RAD50 as a monomer. The peptides were used at 50 μM and potassium chloride, instead of sodium chloride, was used at 100 mM.

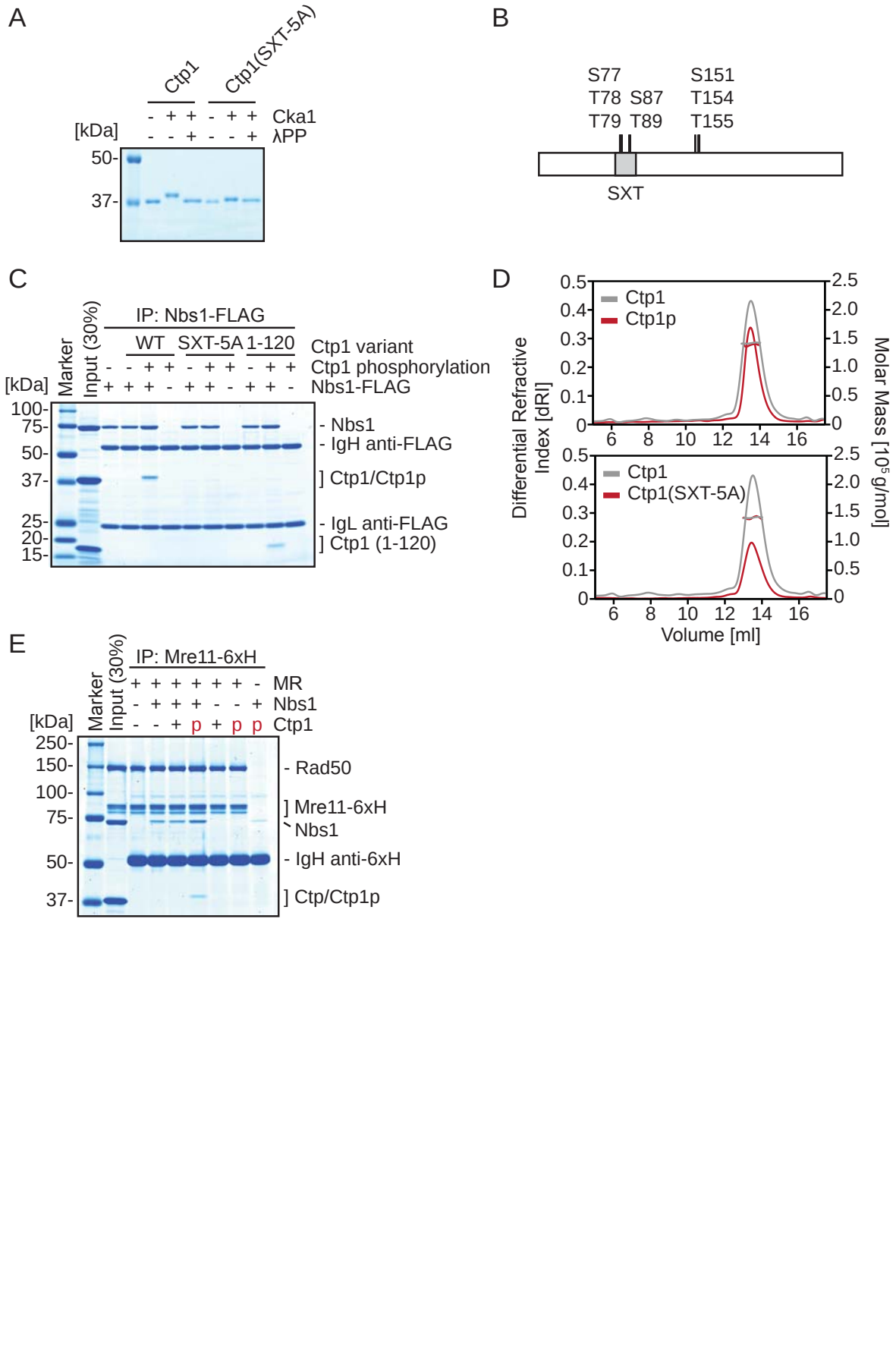
A
Ctp1
Ctp1(SXT-5A)
Cka1
λPP
[kDa]
50-
37-
B
S77
T78 S87
T79 T89
S151
T154
T155
SXT
C
IP: Nbs1-FLAG
WT
SXT-5A
1-120
Ctp1 variant
Ctp1 phosphorylation
Nbs1-FLAG
Marker
Input (30%)
[kDa]
100-
75-
50-
37-
25-
20-
15-
- Nbs1
- IgH anti-FLAG
] Ctp1/Ctp1p
- IgL anti-FLAG
] Ctp1 (1-120)
D
Ctp1
Ctp1p
Ctp1(SXT-5A)
Differential Refractive Index [dRI]
Molar Mass [10⁵ g/mol]
Volume [ml]
E
IP: Mre11-6xH
MR
Nbs1
Ctp1
Marker
Input (30%)
[kDa]
250-
150-
100-
75-
50-
37-
- Rad50
] Mre11-6xH
Nbs1
- IgH anti-6xH
] Ctp/Ctp1p

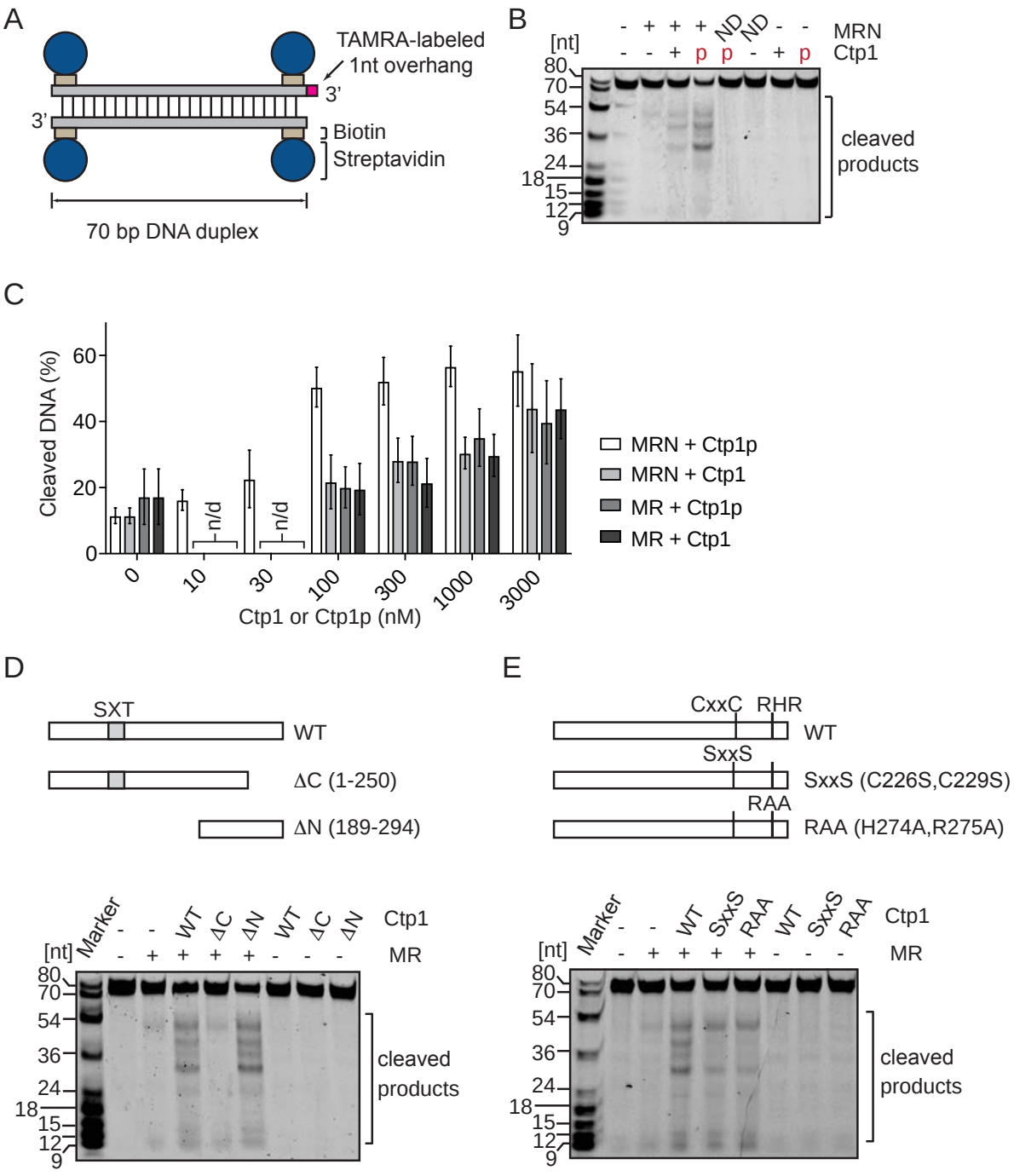
A
TAMRA-labeled
1nt overhang
3'
3'
Biotin
Streptavidin
70 bp DNA duplex
B
[nt]
MRN
Ctp1
ND
ND
cleaved
products
C
Cleaved DNA (%)
n/d
n/d
MRN + Ctp1p
MRN + Ctp1
MR + Ctp1p
MR + Ctp1
Ctp1 or Ctp1p (nM)
D
SXT
WT
ΔC (1-250)
ΔN (189-294)
Marker
Ctp1
MR
cleaved
products
E
CxxC
RHR
WT
SxxS
SxxS (C226S,C229S)
RAA
RAA (H274A,R275A)
cleaved
products

A

Organism	Protein	UniProtKB	C-terminal alignment of Ctp1/CtIP	
S. pombe	Ctp1	O74986	PKPIPNGFWESDFVD*	294
S. cryophilus	CtIP	S9X4T5	PKRIPDGFWESDFVD*	297
S. cerevisiae	Sae2	P46946	RSKSPPGFGRLDFPSTQ	280
A. thaliana	GR1	Q9ZRT1	PPMTPEGFWNIGFESEM	588
D. melanogaster	CtIP	Q9VPF5	RSSTPPGFWNPHMVSFA	474
D. rerio	RBBP8	F1R983	PPSTPENFWEVGFPSTQ	630
X. laevis	CtIP	Q6GNV6	PPSTPENFWEVGFPSTQ	819
G. gallus	RBBP8	E1C2F1	PPNTPENFWEVGFPSTQ	875
M. musculus	CtIP	Q80YR6	PPNTPENFWEVGFPSTQ	856
H. sapiens	CtIP	Q99708	PPNTPENFWEVGFPSTQ	860

CDK ATM

B

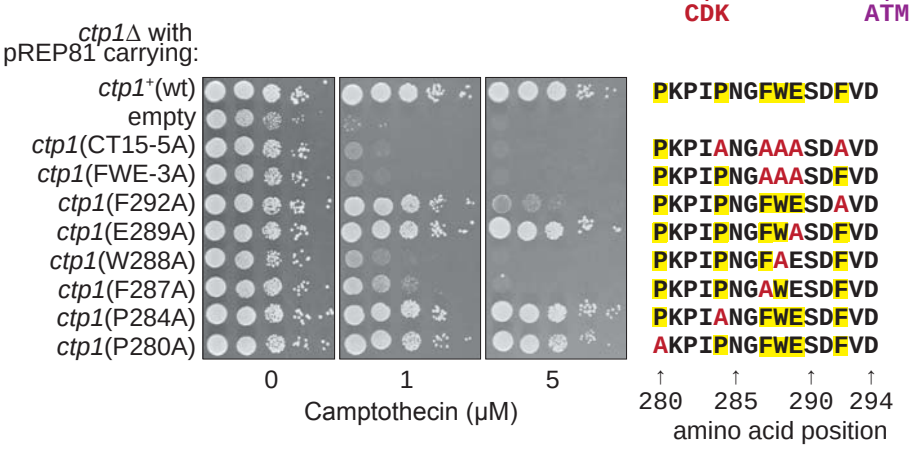

C

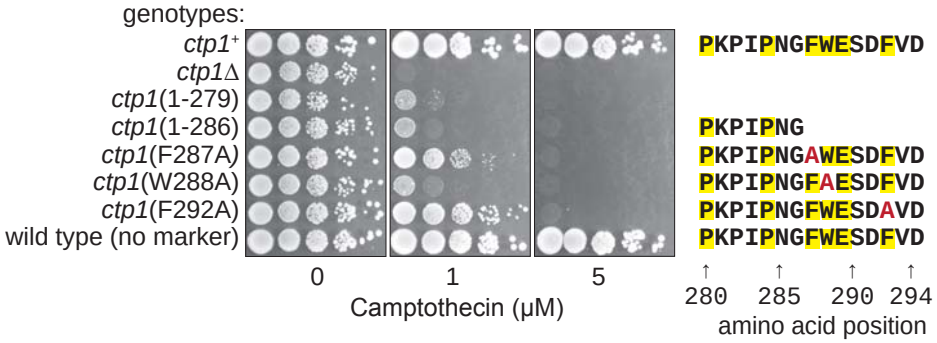

D

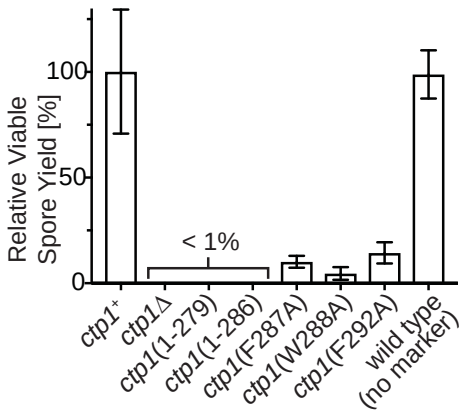

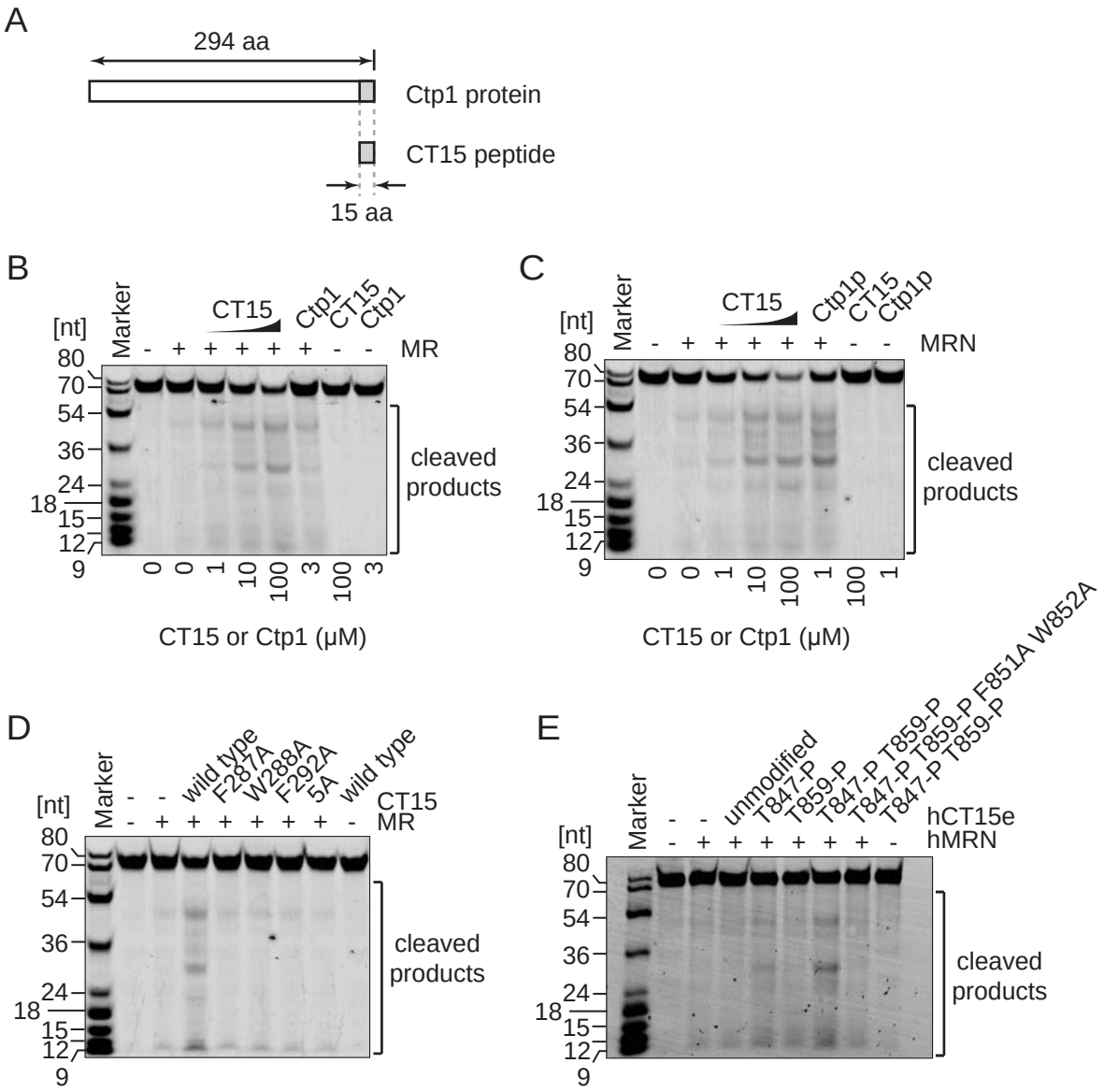
A
294 aa
Ctp1 protein
CT15 peptide
15 aa
B
[nt]
Marker
CT15
Ctp1
CT15
Ctp1
MR
80
70
54
36
24
18
15
12
9
cleaved products
0 0 1 10 100 3 100 3
CT15 or Ctp1 (μM)
C
[nt]
Marker
CT15
Ctp1p
CT15
Ctp1p
MRN
cleaved products
0 0 1 10 100 1 100 1
CT15 or Ctp1 (μM)
D
[nt]
Marker
wild type
F287A
W288A
F292A
5A
wild type
CT15
MR
cleaved products
E
[nt]
Marker
unmodified
T847-P
T859-P
T847-P T859-P
T847-P T859-P F851A W852A
T847-P T859-P
hCT15e
hMRN
cleaved products

Supplementary Information for

A Conserved Ctp1/CtIP C-Terminal Peptide Stimulates Mre11 Endonuclease Activity

Aleksandar Zdravković[1,2], James M. Daley[3], Arijit Dutta[3], Tatsuya Niwa[1,2], Yasuto Murayama[4], Shuji Kanamaru[1,2], Kentaro Ito[2], Takahisa Maki[2], Bilge Argunhan[2], Masayuki Takahashi[1], Hideo Tsubouchi[1,2]*, Patrick Sung[3]*, Hiroshi Iwasaki[1,2]*.

[1]School and Graduate School of Bioscience and Biotechnology, Tokyo Institute of Technology, 4259 Nagatsuta, Midori-ku, Yokohama, Kanagawa 226-8503, Japan.
[2]Institute of Innovative Research, Tokyo Institute of Technology, 4259 Nagatsuta, Midori-ku, Yokohama, Kanagawa 226-8503, Japan.
[3]Department of Biochemistry and Structural Biology, University of Texas Health Science Center, San Antonio, TX 78229, USA.
[4]Center for Frontier Research, National Institute of Genetics, 1111 Yata, Mishima, Shizuoka 411-8540, Japan.

*Correspondence to: htsubouchi@bio.titech.ac.jp, sungp@uthscsa.edu, hiwasaki@bio.titech.ac.jp

This PDF file includes:

Supplementary text
Figures S1 to S5
Tables S1 to S3
SI References

Supplementary Information Text

SI Materials and Methods

Schizosaccharomyces pombe strain manipulation

Standard procedures were used for culturing and genetic manipulation of strains (1). The *S. pombe* strains used in this study are shown in SI Appendix, Table S2.

Viable spore yield assay

Viable spore yield assays were performed as described previously (2). Briefly, 1.2 x 10^6 cells of strain h^- cells carrying *ctp1* variants (spAZ_114, spAZ_120, spAZ_123, spAZ_128, spAZ_0132, or spAZ_134) was crossed with an excess of h^+ *ctp1*Δ cells (YA1097: h^+, *his3-D1*, *leu1-32*, *ura4-D18*, *ade6-M210*, *ctp1*Δ::*ura4*$^+$) (3) on SPA sporulation agar. The mating mixtures were allowed to undergo meiosis at 25°C. Cells were harvested after 2–3 days and treated with glusulase and ethanol to kill vegetative cells. The cell mixture was then plated on yeast extract agar (YEA) and the number of colonies were counted after 2-3 days of incubation at 30°C. Viable spore yield was expressed as a percentage for each h^- query strain, with 100% equal to the number of colonies obtained with the h^- *ctp1*$^+$ control strain (YA119).

Oligo primers for PCR

Primers used in this study are listed in SI Appendix, Table S3.

Expression and purification of the Mre11-Rad50 (MR) complex

The *mre11*$^+$ cDNA on pBluescript II SK (+) (4) was subcloned to enable expression of the protein from the *GAL1/10* promoter in the pESC-Ura plasmid (Agilent Technologies), giving pESC-Mre11. The PSOL10009 primer introduced a 6×His tag at the C-terminus of Mre11. The *rad50*$^+$ cDNA was amplified using PSOL10010 and PSOL10011 and cloned into pESC-Trp (Agilent Technologies), giving pESC-Rad50. The two resultant plasmids were introduced into the protease-deficient *Saccharomyces cerevisiae* strain YRP654 (5). Cultures were grown overnight to stationary phase in SC medium lacking Ura and Trp (SC Ura$^-$ Trp$^-$) and diluted eightfold into SC Ura$^-$ Trp$^-$ media with 3% glycerol, 3% lactic acid, and 2% galactose. After 24 h of growth at 30°C, cells were harvested by centrifugation, immediately snap-frozen as small pellets in liquid nitrogen, and then ground to a fine powder under liquid nitrogen using a 6875 Freezer/Mill Cryogenic Grinder (SPEX, NJ, USA). The cell powder was stored at –80°C until required. About 20 g frozen cell powder was then suspended in 100 ml crude-

extract buffer (20 mM potassium phosphate [pH 7.5], 300 mM KCl, 10% glycerol, 0.05% polysorbate 20, 1 mM 2-mercaptoethanol, 0.5 mM phenylmethylsulfonyl fluoride [PMSF], and protease inhibitor cocktail [Roche]) at room temperature. As soon as the cell powder was suspended, the suspension was immediately put on ice. Subsequent steps were performed at 0–4°C. The cell suspension was centrifuged at 186,000 × *g* for 2 h in a Ti45 rotor (Beckman). The cleared supernatant was mixed with 4 ml Ni-NTA Superflow resin (Qiagen) in a capped test tube, which was gently rotated for 3 h. The slurry was poured into a 1 cm diameter disposable column, and the packed resin was slowly washed with a series of four different buffers in the following order: 300 ml buffer A (20 mM potassium phosphate [pH 7.5], 500 mM KCl, 1 mM ATP, 8 mM $MgCl_2$, 10% glycerol, 0.05% polysorbate 20, and 1 mM 2-mercaptoethanol, 30 mM imidazole), 100 ml buffer B (20 mM Tris-Cl [pH 8.0], 300 mM KCl, 1 mM ATP, 8 mM $MgCl_2$, 10% glycerol, 0.05% polysorbate 20, and 1 mM 2-mercaptoethanol, 30 mM imidazole), 100 ml buffer C (20 mM potassium phosphate [pH 7.0], 300 mM KCl, 1 mM ATP, 8 mM $MgCl_2$, 10% glycerol, 0.05% polysorbate 20, and 1 mM 2-mercaptoethanol, 30 mM imidazole), and 10ml buffer D (20 mM potassium phosphate [pH 7.5], 100 mM KCl, 10% glycerol, 0.05% polysorbate 20, and 1 mM 2-mercaptoethanol). The resin was resuspended in 15 ml elution buffer (20 mM potassium phosphate [pH 7.5], 100 mM KCl, 300 mM imidazole, 10% glycerol, 0.05% polysorbate 20, and 1 mM 2-mercaptoethanol) in the same column, which was capped to prevent leakage, and rotated continuously for ~15 h. The flow-through fraction, obtained by passing through the column, was diluted with 45 ml buffer E (20 mM potassium phosphate [pH 7.5], 10% glycerol, 0.05% polysorbate 20, 1 mM 2-mercaptoethanol, and 0.5 mM EDTA). The diluted sample was applied to a 5 ml Heparin HP column (GE Healthcare), pre-equilibrated with buffer E containing 100 mM KCl. The column was washed with 30 ml buffer E containing 200 mM KCl, and the proteins that were bound to the resin were eluted with a linear gradient of 200 mM to 1 M KCl in 20 ml buffer E. Peak fractions containing MR complex, as determined by western blotting with anti-His-tag antibody, were loaded onto a HiLoad 26/600 Superdex 200 pg (GE Healthcare) size-exclusion column pre-equilibrated with buffer F (20 mM Tris-Cl [pH 7.5], 10% glycerol, 0.05% polysorbate 20, 1 mM 2-mercaptoethanol, and 0.5 mM EDTA) containing 300 mM NaCl, and proteins were eluted with the same buffer. MR complex eluted at ~110–120 ml, separately from free Mre11, which eluted at ~130–150 ml. Fractions containing MR complex were diluted with two volumes of buffer F and applied to a 1 ml RESOURCE Q anion-exchange column (GE Healthcare). Proteins were eluted with a linear gradient of 50 mM to 1 M NaCl in 9 ml buffer F. Peak fractions containing MR complex were diluted to a final concentration of 100 mM NaCl with buffer F and concentrated by Amicon Ultra-4 10K Centrifugal Filters (Merck Millipore) to 0.3–1 mg/ml MR. The concentrated sample was dispensed into small aliquots,

snap-frozen in liquid nitrogen, and stored at –80°C until required.

cDNA corresponding to the nuclease-deficient Mre11^{H134R} was made with the QuikChange II kit (Agilent) with two primers, oAZ_94 and oAZ_95, and pESC-Mre11 as the template. Expression and purification of the M^{H134R}R complex was carried out by the same procedure as for the wild-type MR complex. The M^{H134R}R complex behaved identically to wild-type MR during purification.

Expression and purification of Nbs1

For the purification of Nbs1 from insect cells, the *nbs1*$^{+}$ cDNA on pNT140 (3) was subcloned into a pFastBac vector, giving pFastBac-Nbs1. The PSOL9975 primer introduced a FLAG tag at the C-terminus of Nbs1. Bacmid, transfected Sf9 cells, and viruses were prepared according to the manufacturer's instructions (Bac-to-Bac, Invitrogen). High-titer virus was transfected into Sf9 cells (2 × 10^{6} cells/ml) in 800 ml cell culture. After incubation for 45 h at 27°C, cells were harvested by centrifugation (700 × *g* for 10 min), washed in phosphate-buffered saline, snap-frozen in liquid nitrogen, and stored at –80°C until further use.

All purification steps were performed at 4°C. Cells were resuspended and stirred gently in 8 ml swelling buffer (50 mM Tris-HCl [pH 7.5], 2 mM DTT) for 30 min. The following were added to the cell suspension: protease inhibitors (aprotinin, chymostatin, leupeptin, and pepstatin at final concentrations of 5 *μ*g/ml each, and PMSF at a final concentration of 0.5 mM), 1 ml of 50% glycerol, and 4 M NaCl up to a final NaCl concentration of 300 mM. The suspension was stirred for 30 min, followed by centrifugation at 186,000 × *g* in a Ti45 rotor (Beckman) for 1 h. The supernatant was collected and mixed with 3 ml settled Anti-FLAG M2 Affinity Gel (Sigma) in a bottle, which was rotated for 2.5 h. The slurry was poured into a 1 cm diameter disposable column, and the packed resin was slowly washed with 200 ml T buffer (25 mM Tris-HCl [pH 7.5], 10% glycerol, 0.01% IGEPAL CA-630 [MP medical], and 1mM DTT) containing 500 mM KCl. The resin was incubated with 6 ml of 0.2 mg/ml 3×FLAG peptide (APExBIO) in 50 mM NaCl T buffer for 20 min to elute the proteins that were bound to the resin. The elution procedure was repeated twice. Eluted fractions were loaded onto a 5 ml HiTrap SP column (GE Healthcare). Proteins were eluted with a linear gradient of 100–500 mM NaCl in 50 ml buffer T. Nbs1-FLAG eluted with a peak corresponding to 360 mM NaCl. The peak fractions containing Nbs1-FLAG were diluted to 100 mM NaCl concentration with buffer T and concentrated using an Amicon Ultra-4 10K Centrifugal Filter (Merck Millipore).

For the purification of Nbs1-FLAG from *Escherichia coli*, the Nbs1-FLAG coding sequence in pFastBac-Nbs1 was introduced into the pBKN220 vector (a high-copy-number pET21a derivative) using the In-Fusion HD cloning kit (Takara) as described by the

manufacturer (with primers oAZ_203, oAZ_204, oAZ_205, and oAZ_206), giving pBKN-Nbs1-FLAG. The pBKN-Nbs1-FLAG plasmid was linearized by PCR with oAZ_265 and oAZ_266 primers, and a human rhinovirus 3C protease site and a 6×His tag were added at the C-terminus of Nbs1-FLAG. The resultant plasmid was named pBKN220-Nbs1-FLAG-3C-His and was introduced into the T7-expression host *E. coli* BL21-CodonPlus (DE3). Bacterial expression of Nbs1-FLAG-3C-His was performed by the auto-induction method at 30°C overnight (6).

E. coli cells were harvested by centrifugation (6,500 × *g* for 15 min), snap-frozen in liquid nitrogen, and stored at –80°C until required. All purification steps were performed at 4°C. A frozen pellet (~1 g) was resuspended in 10 ml extraction buffer (40 mM Tris [pH 8.0], 300 mM NaCl, 10% glycerol, 0.01% IGEPAL CA-630 [MP medical], 1 mM DTT, protease inhibitor cocktail [Roche], and 0.5 mM PMSF), followed by sonication (BRANSON Digital Sonifier 250, 20 kHz, 12.5 mm flat tip, 30% amplitude, 15 min on time, 0.5 s on / 1 s off pulse, 5°C temperature limit) and ultra-centrifugation (72,000 × *g* for 1 h). Ni-NTA Superflow resin (5 ml of slurry, Qiagen) was added to the crude extract in a bottle, which was rotated for 2.5 h. The resin was poured into a 1 cm diameter disposable column and slowly washed with 200 ml T buffer containing 25 mM imidazole and 500 mM KCl. Nbs1-FLAG-3C-His was eluted with 15 ml T buffer containing 360 mM imidazole and 100 mM NaCl. PreScission protease (GE Healthcare) was added to the eluted fraction, following the manufacturer's guidelines. The sample was then dialyzed against T buffer containing 90 mM NaCl, and the dialyzate was loaded onto a HiLoad 26/600 Superdex 200 prep-grade column (GE) that was pre-equilibrated with T buffer containing 100 mM NaCl. Proteins were eluted with T buffer containing 100 mM NaCl; fractions corresponding to 155–165 ml elution volume contained Nbs1-FLAG, and were pooled, concentrated with an Amicon Ultra-4 3K Centrifugal Filter (Merck Millipore), snap-frozen, and stored at –80°C until use.

Nbs1-FLAG proteins purified from insect cells and bacterial cells were judged to have the same properties.

Expression and purification of GST-Cka1

The *cka1*$^{+}$ cDNA was cloned into a pGEX-6P-1N plasmid, giving pGST-Cka1. GST-Cka1 fusion protein was expressed in *E. coli* BL21-CodonPlus (DE3) cells using the auto-induction method at 30°C for ~15 h (6). *E. coli* cells were harvested by centrifugation (6,500 × *g* for 15 min), snap-frozen in liquid nitrogen, and stored at –80°C until use. All purification steps were performed at 4°C. A frozen pellet (~1 g) was resuspended in lysis buffer (40 mM Tris-Cl [pH 7.5], 300 mM KCl, 1 mM DTT, 0.05% polysorbate 20 (MP Biomedical), protease-inhibitor cocktail (Roche), and 0.5 mM PMSF), followed by sonication (BRANSON Digital Sonifier 250,

20 kHz, 12.5 mm flat tip, 30% amplitude, 15min on time, 0.5 s on / 1 s off pulse, 5°C temperature limit) and ultra-centrifugation (75,000 × *g* for 1 h). Glutathione Sepharose 4B resin (5 ml slurry, GE Healthcare) was added to the crude extract in a bottle, which was rotated for 2 h. The resin was applied to a disposable 1 cm diameter column and slowly washed with 100 ml buffer T containing 25 mM imidazole and 500 mM KCl. The GST-Cka1 was eluted with 15 ml T buffer containing 50 mM glutathione and 50 mM KCl. The eluate was loaded directly onto a 1 ml HiTrap Heparin HP column. Proteins were eluted with a linear gradient of 200–700 mM KCl in 10 ml T buffer. Peak fractions containing GST-Cka1 (corresponding to ~475 mM KCl) were concentrated in an Amicon 30k unit (Millipore), snap-frozen, and stored at –80°C.

Expression and purification of Ctp1 and its derivatives

ctp1^{+} cDNA was cloned into pBKN220, giving pBKN-Ctp1(original). The first 11 codons of *ctp1* were corrected to the following sequence ATGAACGAAGAAGAACACAACAAATCTGTTCAC using site-directed mutagenesis. This sequence has a higher *E. coli* usage frequency while preserving the same amino-acid sequence. The resultant codon corrected plasmid was named pBKN-Ctp1. BL21-CodonPlus (DE3) *E. coli* cells transformed with pBKN-Ctp1 were grown to $OD_{600} \approx 0.3$ in LB broth at 37°C. Expression of Ctp1 was induced by addition of isopropyl-β-D-thiogalactoside (final concentration, 1 mM). After a 3 h incubation, cells were harvested by centrifugation (6,500 × *g* for 15 min), snap-frozen in liquid nitrogen, and stored at –80°C until required.

All subsequent purification steps were performed at 4°C. A frozen pellet was resuspended in 20 ml R buffer (20 mM Tris-HCl [pH 8.0], 1 mM EDTA, 10% glycerol, and 1 mM DTT) containing 300 mM NaCl, 1 mM PMSF, protease-inhibitor cocktail (Roche), with DTT added to a final concentration of 5 mM. Cells were disrupted by sonication (BRANSON Digital Sonifier 250, 20 kHz, 12.5 mm flat tip, 30% amplitude, 15min on time, 0.5 s on / 1 s off pulse, 4°C temperature limit), and cleared extract was obtained by ultra-centrifugation (67,000 × *g* for 1 h). The sample was diluted with three volumes of R buffer and loaded onto two sequentially connected HiTrap SP HP 5 ml columns (GE Healthcare). Proteins were eluted with a linear gradient of 0–1 M NaCl over the volume of 100 ml R buffer. Peak fractions containing Ctp1 were pooled, adjusted to 2 mM ATP and 10 mM $MgCl_2$, and stirred gently for 1 h. The mixture was diluted with two volumes of R buffer and loaded onto a HiTrap Heparin 5 ml column (GE Healthcare) pre-equilibrated with R buffer containing 100 mM NaCl. Proteins were eluted with a linear gradient of 100–700 mM NaCl over the volume of 60 ml R buffer. Pooled peak fractions containing Ctp1 were diluted by addition of three volumes of R buffer and loaded onto a 1 ml RESOURCE Q column (GE Healthcare). Proteins were eluted

with a linear gradient of 50–500 mM NaCl over the volume of 9 ml R buffer. Peak fractions were diluted with R buffer to adjust the final concentration to 150 mM NaCl, and then were snap-frozen in small aliquots and stored at –80°C until required.

Codon changes within the conserved CxxC motif of Ctp1 resulting in the SxxS mutant were introduced by PCR linearizing the pBKN-Ctp1 plasmid using oAZ_235 an oAZ_236 primers and circularizing the generated fragment by In-Fusion HD cloning kit (Takara). Codons within the Ctp1 RHR motif were changed to RAA by site-directed mutagenesis using the oAZ_087 and oAZ_088 primers and pBKN-Ctp1 as a template. N-terminal truncation of Ctp1 was generated by running a PCR using oAZ_458 and T7 terminator primers on pBKN-Ctp1 as template, with the resulting fragment being ligated into the pBKN backbone following NdeI and BamHI digestion. These Ctp1 variants were purified by the same procedure as for wild-type Ctp1 protein.

C-terminal truncation of Ctp1 was generated by introducing Strep-Tag II via PCR using oAZ_153 & oAZ_158 primers and pBKN-Ctp1 as template followed by circularization of the generated fragment with the In-Fusion HD cloning kit. This protein was expressed in *E. coli*, and crude cell extract was obtained as described for wild-type Ctp1. To the crude extract of Ctp1(1-250)-strep, 1 ml Strep-Tactin Superflow resin (IBA) was added in a bottle, which was mixed slowly at 4°C for 1.5 h. Resin was washed with 100 ml R buffer containing 300 mM NaCl. Elution was performed by addition of 10 ml of 10 mM d-desthiobiotin. The eluate was further purified with a RESOURCE Q column and treated as described in the final step for the wild-type Ctp1 protein.

Preparation and dephosphorylation of *in vitro*-phosphorylated Ctp1 and its derivatives

Phosphorylation reaction mix containing 1 mg/ml Ctp1, 0.004 mg/ml GST-Cka1, 2 mM ATP, 20 mM $MgCl_2$, 50 mM NaCl, and 20 mM Tris-HCl (pH 7.5) was incubated at 30°C for 16 h. Phosphorylated protein was purified by HiTrap SP HP and HiTrap Heparin columns, as described for unphosphorylated Ctp1. Pooled fractions were adjusted to a final concentration of 100 mM NaCl in R buffer, concentrated using Amicon 10k (Millipore) filters, snap-frozen, and stored at –80°C. The same procedure was used for preparation of phosphorylated Ctp1(SXT-5A). Ctp1(1–120) was phosphorylated in the same way but used without the purification procedure. For dephosphorylation, the phosphorylated proteins were treated with Lambda Protein Phosphatase (NEB), as instructed by the manufacturer.

Human MRN purification

Untagged Human MRE11 (hMRE11) and hRAD50 with a C-terminal 6xHis tag were cloned into the ClaI and SmaI sites of pESC-Ura, respectively, to create pJD178. The hMR complex

was expressed by galactose induction in 20 L of the *S. cerevisiae* strain YRP654 (5). Flag-hNBS1 was cloned into pFastBac to create pJD83 and was used to create a baculovirus by transformation into DH10Bac cells. hNBS1 was expressed in High 5 insect cells by infection with this baculovirus and 1 L of cells were harvested after 48 hr. Both the hMR and hNBS1 pellets were broken in K buffer (20 mM KH_2PO_4, 10% glycerol, 0.5 mM EDTA, 0.5% Tween 20, 1 mM β-mercaptoethanol, and protease inhibitors: 1 mM PMSF and 5 mg/mL each of aprotinin, chymostatin, leupeptin, and pepstatin) with 300 mM KCl and spun down in a Beckman ultracentrifuge at 100,000 x *g* for 45 min. The clarified hMR and hNBS1 lysates were incubated with 2 ml of nickel or flag affinity resin, respectively, for 1 hr at 4°C. Each resin was washed sequentially with 15 ml K buffer with 300 mM KCl; 500 ml K buffer with 500 mM KCl, 1 mM ATP, and 8 mM $MgCl_2$; and 15 ml K buffer with 150 mM KCl. Then, the resin was treated five times with 2 ml of K buffer containing 150 mM KCl and, either 200 mM imidazole for hMR or 250 ng/ml of FLAG peptide (Sigma) for hNBS1, for 10 min to elute proteins. The hMR and hNBS1 eluates were mixed and incubated overnight at 4°C to form the hMRN complex. The resulting complex was then fractionated in a 1 ml heparin column (Amersham) with a 50-mL 150–650 mM KCl gradient. The peak was collected, concentrated in an Ultracel-100K device (Amicon), and loaded onto a 24-mL Superose 6 column (GE Healthcare) in K buffer with 250 mM KCl. Peak fractions were concentrated again, frozen in liquid nitrogen in small aliquots, and stored at -80°C.

Mass spectrometry

For mass spectrometry, Ctp1 was partially phosphorylated by incubating 0.33 mg/ml Ctp1 and 0.02 mg/ml GST-Cka1 in reaction buffer (20 mM Tris-HCl [pH 7.5], 20 mM $MgCl_2$, 2 mM ATP, 20 mM NaCl, and 80 mM KCl) for 5 min at 30°C. The phosphorylation reaction was stopped by addition of SDS-PAGE sample-loading buffer. Phosphorylated samples were reduced by addition of 1/10 volume of 250 mM Tris(2-carboxyethyl)phosphine (TCEP), and the samples were incubated for 15 min at room temperature. The samples were then alkylated by addition of a 1/10 volume of 500 mM freshly-made iodoacetamide and incubated at room temperature for 15 min. Samples were separated by 8% SDS-PAGE and stained with Coomassie brilliant blue G-250. Stained protein bands were excised, destained with 30% acetonitrile and 50 mM ammonium bicarbonate (ABC) solution, and dehydrated with 60% acetonitrile and 50 mM ABC solution. Dehydrated gel slices were dried further in a centrifugal evaporator, and then were rehydrated in 50 mM ABC solution containing 12.5 μg/ml Trypsin Gold (Promega) and incubated at 37°C overnight for digestion. The digested peptides were extracted in 50% acetonitrile, dried in a centrifugal evaporator, dissolved in 2% acetonitrile and 0.1% TFA solution, and desalted with a C18 Stage Tip (Nikkyo Technos).

After desalting, the peptide solution was dried in a centrifugal evaporator. The peptides were re-dissolved in 2% acetonitrile and 0.1% TFA solution, and subjected to nanoLC–MS/MS measurement on an Easy-nLC 1000 nanoLC system and a Q-Exactive mass spectrometer (ThermoFisher Scientific). The settings used have been described previously (7), except that the gradient condition of nanoLC was set as 10–40% at 30 min. MS/MS spectra were searched against the amino-acid sequences of *S. pombe* proteome obtained from UniProt Database (UP000002485) by using the Sequest HT algorithm within Proteome Discoverer 2.4 (Thermo Fisher Scientific). To detect phosphorylation sites, +79.966 Da dynamic modification was set at Ser, Thr and Tyr. The measurement was performed three times per each sample, and the three raw files were merged into one analysis data on Proteome Discoverer.

Co-immunoprecipitation

Mre11(6×His)-Rad50 (2.25 μg), Nbs1-FLAG (0.7 μg), and Ctp1 (1.5 μg) were mixed in 15 μl IP buffer (20 mM Tris-HCl [pH 7.5], 150 mM NaCl, 3 mM $MgCl_2$, 2.5% glycerol, 0.5% IGEPAL CA-630 [MP Biomedical]), and then incubated on ice for 20 min. The reaction was then mixed with 135 μl Surebeads Protein G (Biorad), pre-treated with anti-6×His monoclonal antibody 28-75 (Wako, 014-23221) or with anti-FLAG M2 antibody (Sigma, F3165), in IP-BSA buffer (IP buffer containing 0.1mg/ml BSA). The mixtures were gently agitated at 4°C for 3 h, washed three times with IP buffer. and the proteins bound to the beads were eluted by boiling in SDS loading buffer and then analyzed by 8% SDS-PAGE.

DNA substrates

Double-stranded DNA made by annealing with oAZ_294 (5'-G**T**AAG TGCCG CGGTG CGGGT GCCAG GGCGT GCCCT TGGGC TCCCC GGGCG CGTAC TCCAC CTCAT GCA**TC**-3') and oAZ_295 (5'-GATGC ATGAG GTGGA GTACG CGCCC GGGGA GCCCA AGGGC ACGCC CTGGC ACCCG CACCG CGGCA CTTAC-3') (Eurofins Genomics, USA), where bold "**T**" and bold "**C**" represents the position of conjugation of biotin and TAMRA, respectively, were used for the endonuclease assay. oAZ_294 and oAZ_295 correspond to the sequence of PC210 and PC211 as described previously by Pinto et al (8), respectively, except for the addition of the TAMRA conjugated "**C**" as a single nucleotide overhang. The two oligonucleotides were annealed in a thermal cycler (~0.3°C/min linear temperature gradient starting from 95°C). For exonuclease assays, dsDNA was used, which was made by annealing of oAZ_135 (**A**AATGAACATAAAGTAAATAAGTC) and oAZ_136 (GACTTATTTACTTTATGTTCATTT) (Integrated DNA Technologies, USA), bold "**A**" denotes the attachment of TAMRA dye to the 5' phosphate.

Exonuclease assay

Standard exonuclease assays were performed in reaction mixture containing 50 mM NaCl, 20 mM Tris-HCl [pH 7.5], 10% glycerol, 1 mM DTT, 0.5 mM $MnCl_2$, 5mM $MgCl_2$, 50 nM DNA, 50 nM $(Mre11)_2(Rad50)_2$, 100 nM Nbs1, and 100 nM Ctp1 variants in terms of monomers. The assays followed the same procedures as the endonuclease assays.

ATPase assay

DNA used in ATPase assays was prepared by annealing oAZ_454 (5'-GTAAG TGCCG CGGTG CGGGT GCCAG GGCGT GCCCT TGGGC TCCCC GGGCG CGTAC TCCAC CTCAT GCATC-3') and oAZ_455 (5'-GATGC ATGAG GTGGA GTACG CGCCC GGGGA GCCCA AGGGC ACGCC CTGGC ACCCG CACCG CGGCA CTTAC-3') (Eurofins Genomics, Japan). Assays were performed in reaction mixture containing 150 mM NaCl, 20 mM Tris-Cl [pH 7.5], 10% glycerol, 1 mM DTT, 0.5 mM $MnCl_2$, 5 mM $MgCl_2$, 150 nM DNA, 0.2 mM ATP, 150 nM $(Mre11)_2(Rad50)_2$, 300 nM Nbs1, and 300 nM Ctp1. Aliquots (2 μl) were taken at designated timepoints and mixed with equal volumes of ice-cold 25 mM EDTA [pH 8.0] (stop reagent) and kept on ice until all aliquots were collected. ATPase activity was determined with a malachite-green assay kit (POMG-25H, Funakoshi), as instructed by the manufacturer.

SEC-MALS analysis

Wild-type (67 μg), phosphorylated wild-type (50 μg) and SXT-5A (30 μg) Ctp1 variants were loaded onto the preequilibrated Superose 6 Increase 10/300 gel filtration column (GE) and eluted isocratically with the same buffer (100mM NaCl, 20mM TRIS, pH 7) at 0.5 ml / min. The column was connected in-line with a DAWN EOS light-scattering and Optilab rex differential refractive index detectors (Wyatt Technology). Data was analyzed by using the ASTRA 5.3.4.20 software (Wyatt Technology).

Synthetic peptides

All peptides were ordered from Toray Research Center (Japan).

Acknowledgments: We thank Yumiko Kurokawa for help with protein purification. We are grateful to members of the Iwasaki laboratory for discussion and encouragement.

Funding: This study was supported in part by the Japan Society for the Promotion of Science, Grants-in-Aid for Scientific Research on Innovative Areas (15H059749 to H.I.), for Scientific Research (A) (18H03985 to H.I.), for Young Scientists (B) (17K15061 to B.A.), for Scientific Research (B) (18H02371 to H.T. and 19H03160 to Y.M.), for Early-Career Scientists (19K16039 to K.I. and 20K15713 to B.A.) and by US National Institutes of Health grant R35 CA241801 (to P.S.).

Competing interests: The authors declare no competing interests.

Author contributions: A.Z., P.S., and H.I. conceived and designed the study. J.M.D. and A.D. purified the human MRN complex. K.I. and T.M. helped with all other protein purifications. T.N. performed MS experiments. A.Z. performed all other experiments. A.Z. and T.N. analyzed MS data. A.Z., J.M.D., A.D., Y.M., S.K., K.I., T.M., B.A., M.T., H.T., P.S., and H.I. analyzed all other data. Y.M., S.K., K.I., T.M., B.A., M.T., H.T., P.S., and H.I. provided expertise and reagents. Y.M., S.K., M.T., H.T., P.S., and H.I. supervised the study. A.Z., T.N., Y.M., B.A., H.T., P.S., and H.I. contributed to writing the manuscript.

Data and materials availability: All data are available in the main text or supplementary materials.

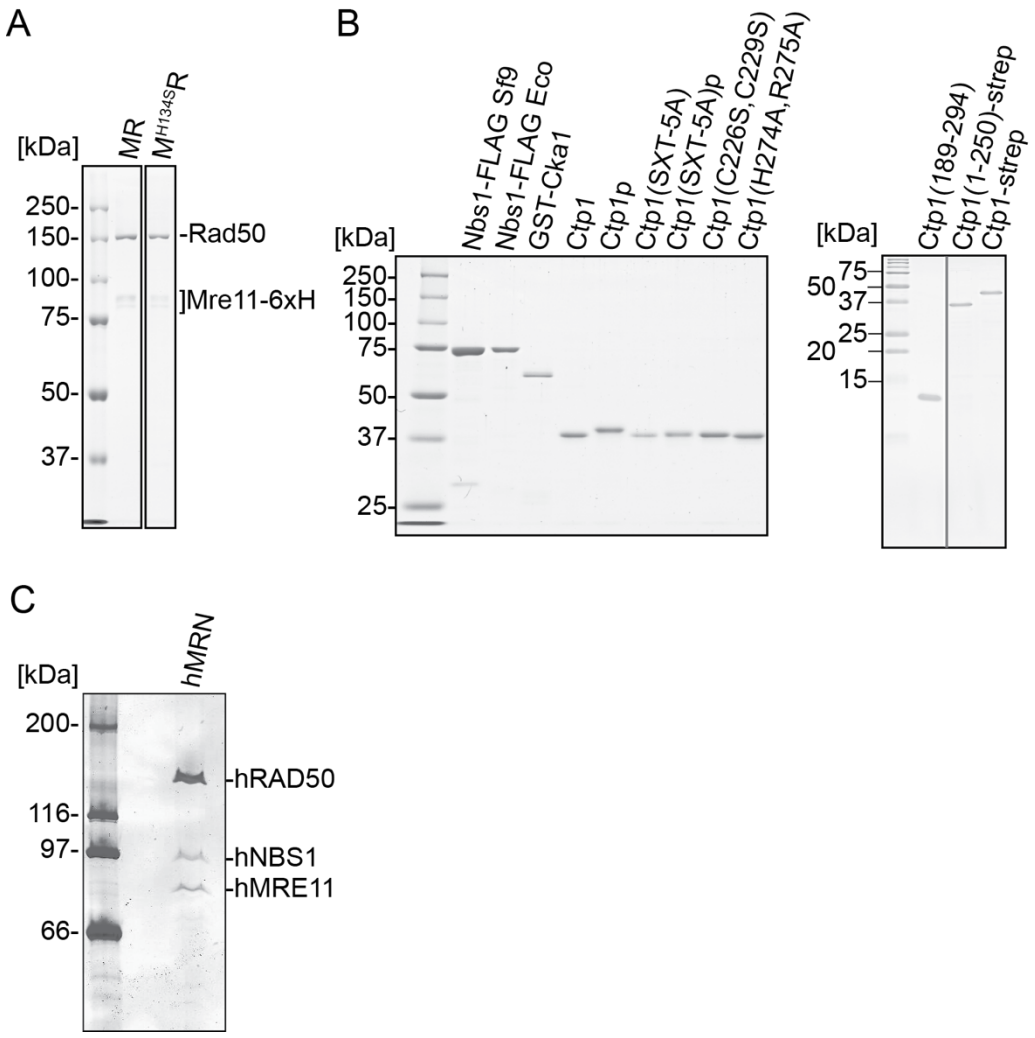

Fig. S1. SDS-PAGE gel image of purified proteins used in this study.

(A) MR complex and nuclease dead Mre11-Rad50 complex. (B) Nbs1, Cka1 and Ctp1 derivatives. (C) Human MRN complex.

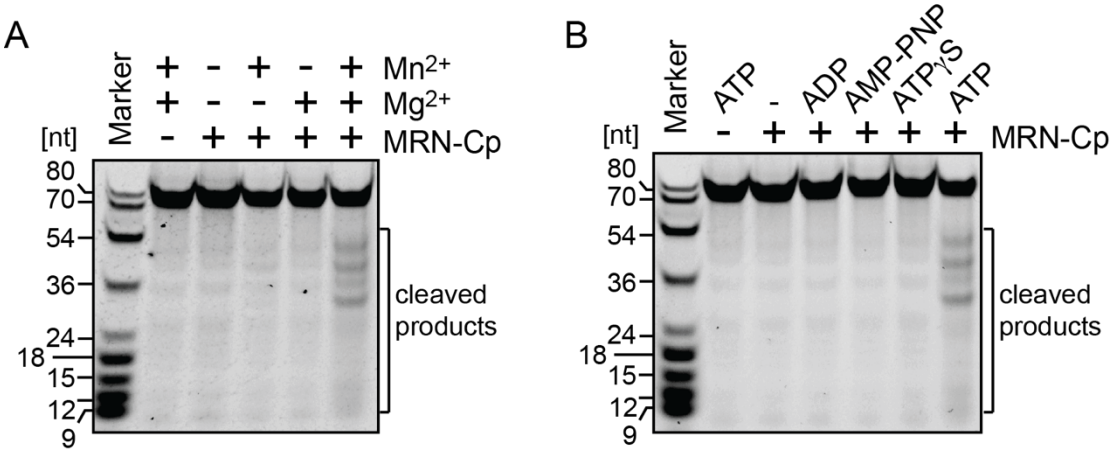

Fig. S2. Requirement for Mre11 endonuclease activity. (A) Both Mg^{2+} and Mn^{2+} are required for Mre11 endonuclease activity in the phosphorylated Ctp1-MRN complex. (B) ATP hydrolysis is required for Mre11 endonuclease in the phosphorylated Ctp1-MRN complex.

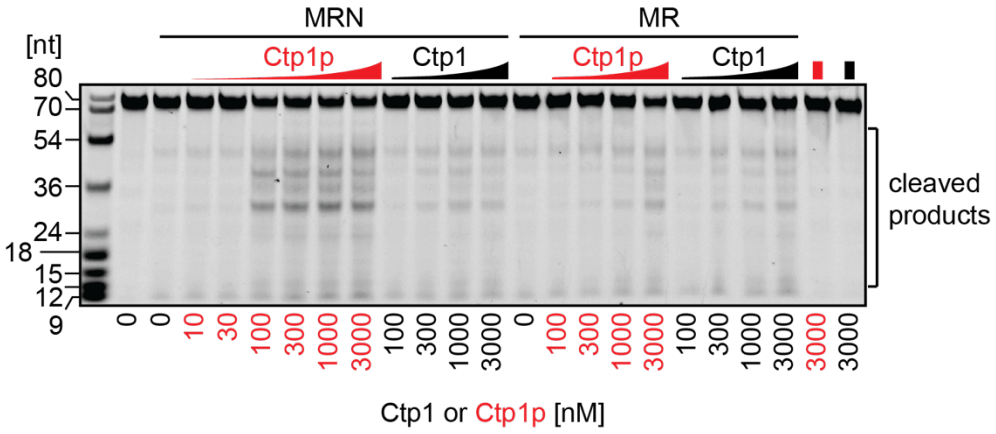

Fig. S3. Titration of Ctp1 in the Mre11 endonuclease assay.

Various concentrations of Ctp1 were included in the Mre11 endonuclease assay in reactions containing Mre11-Rad50-Nbs1 (MRN) or Mre11-Rad50 (MR). Representative gel image used for the quantification shown in Fig. 2C.

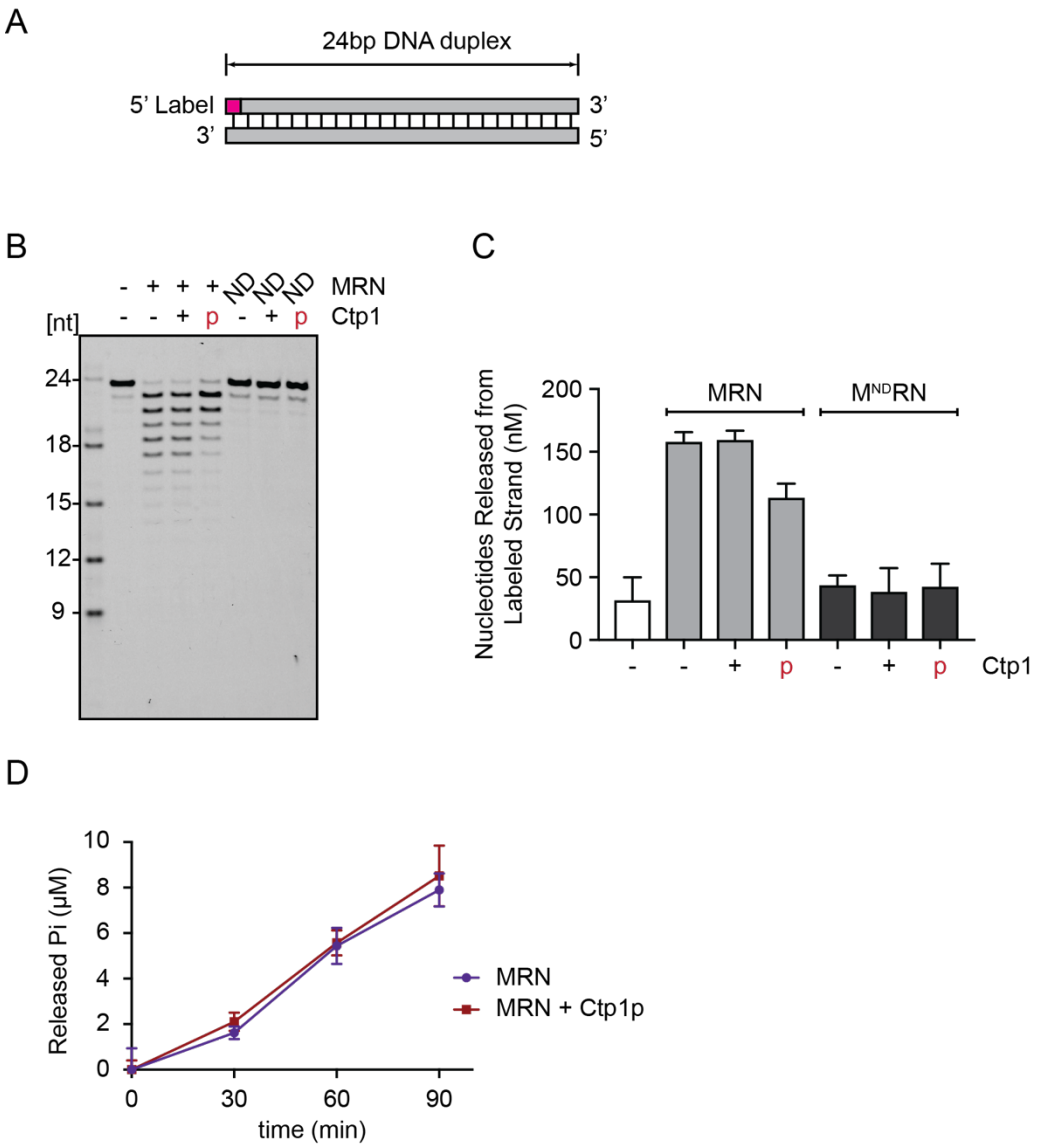

Fig. S4. The effect of phosphorylated Ctp1 (Ctp1-P) on the exonuclease and ATPase activities of MRN.

(A) Illustration of the substrate employed to assay Mre11 exonuclease activity. (B) Mre11 exonuclease activity is not stimulated by Ctp1 and is slightly inhibited by phosphorylated Ctp1. Representative gel image. Proteins were added at equimolar protein-monomer concentrations (100 nM) and incubated at 30°C for 60 min. Red "p" indicates phosphorylated Ctp1. ND indicates MRN complex containing nuclease-deficient Mre11^{H134S}, Rad50, and Nbs1. (C) Quantification of three independent sets of the exonuclease assay shown in (B). Error bars indicate standard deviation, n = 3. (D) Time course of the ATPase activity of MRN demonstrates that phosphorylation of Ctp1 does not affect ATPase activity.

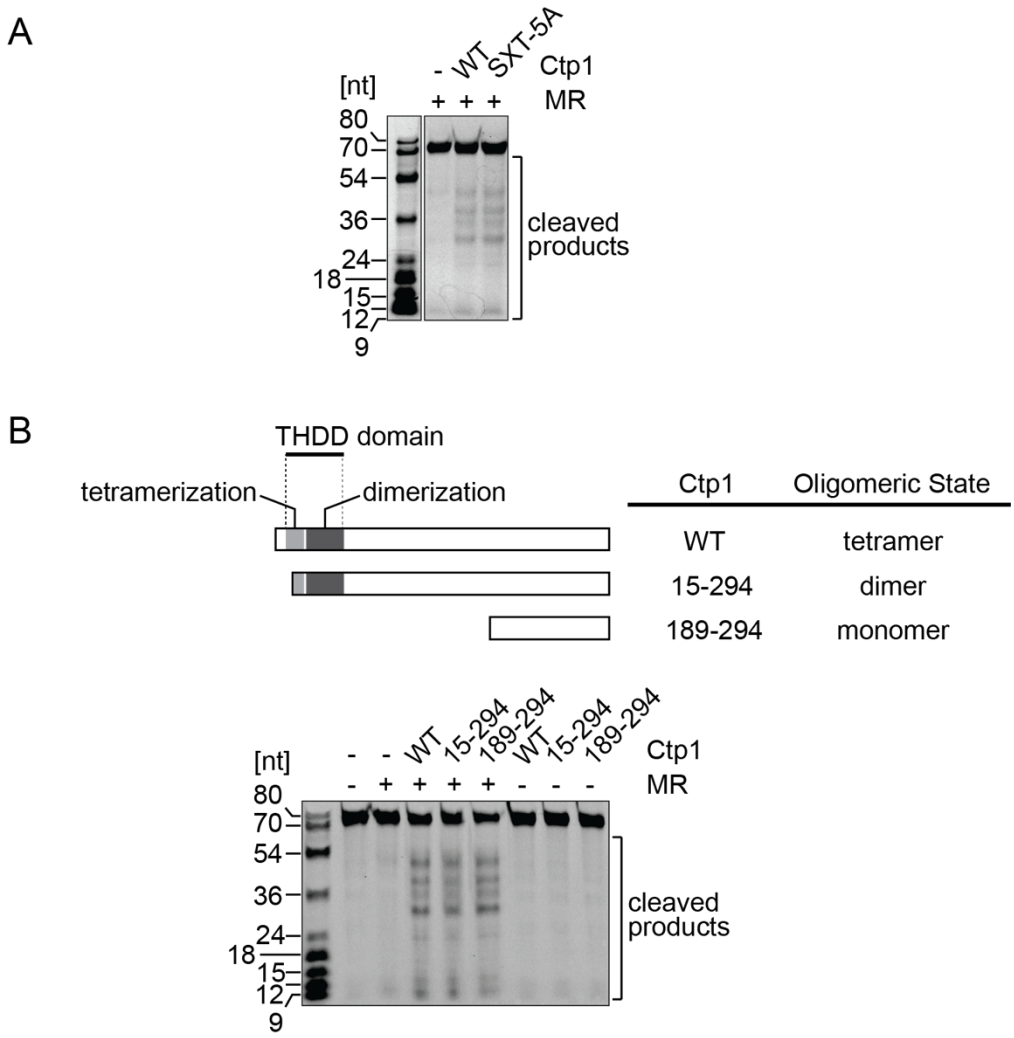

Fig. S5. SXT-5A and mutations that change the oligomeric status of Ctp1 can stimulate MR endonuclease activity.

SXT-5A (A), dimer (15-294) and monomer (189-94) mutants (B) were examined for their ability to stimulate MR endonuclease activity. Ctp1, wild type or variants, at 3 μM.

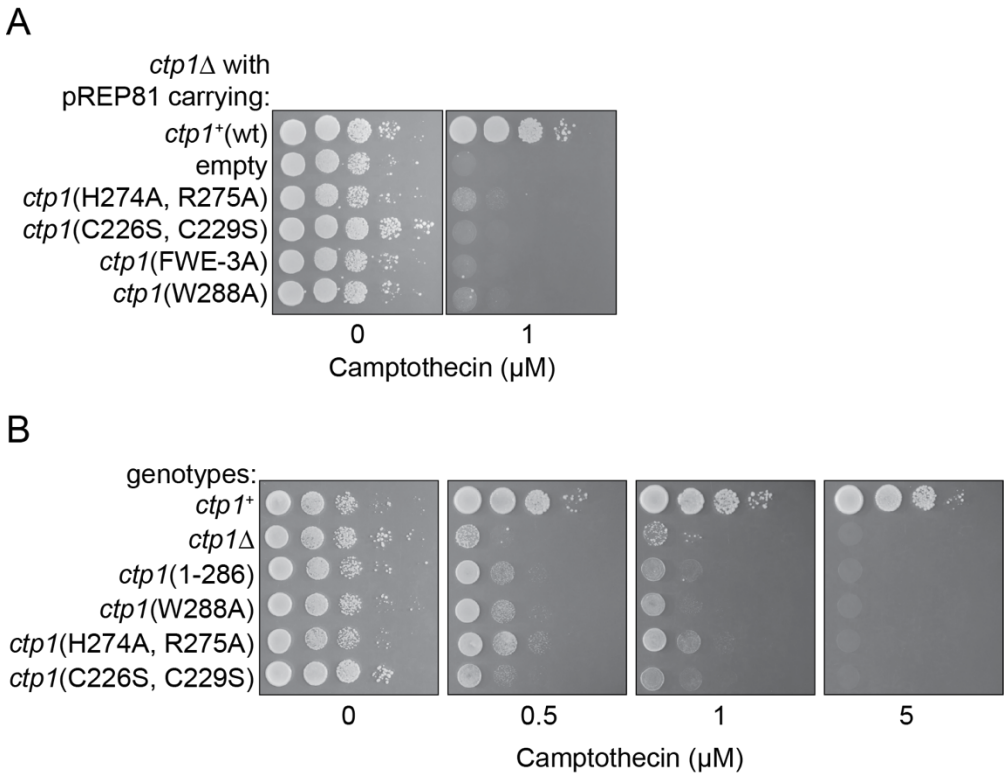

Fig. S6. CxxC and RHR mutants show severe sensitivity to camptothecin.

(A) Complementation of *ctp1Δ* camptothecin sensitivity with plasmids expressing Ctp1 variants. (B) Camptothecin sensitivity of strains with mutations in CxxC or RHR motifs at the endogenous *ctp1* locus. Serially diluted cells were spotted onto YES plates containing the indicated concentration of camptothecin.

Table S1. Ctp1 phosphorylation site analysis

Peptide Sequence	Position in Amino acid sequence	Sample	Number of PSMs	Modifications in Proteins	Theo MHplus in Da	Confidence by Search Engine Sequest HT	Percolator q-Value by Search Engine Sequest HT	Percolator PEP by Search Engine Sequest HT	XCorr by Search Engine Sequest HT
VSSNTIQELDSTTDEDEIPGSDTVDEEDPSLNAPFSEK	67-104	Ctp1	156	(no modification)	4110.8157	High	0.000211	1.61E-08	3.61
		Ctp1p (5min)	66	(no modification)	4110.8157	High	0.0002365	1.60E-09	3.58
			36	1xPhospho [T89(100)]	4190.78203	High	0.0002365	2.52E-08	3.68
			8	2xPhospho [T89(96.3); S/T]	4270.74836	High	0.0002365	1.71E-07	4.16
			2	3xPhospho [T89(97.9); S/T]	4350.7147	High	0.0002365	1.44E-06	4.29
		Ctp1p (full)	28	(no modification)	4110.8157	High	0.0002508	4.78E-08	4.42
			15	1xPhospho [T89(100)]	4190.78203	High	0.0002508	2.76E-07	3.11
			4	2xPhospho [S/T]	4270.74836	High	0.0002508	5.27E-09	4.92
			1	3xPhospho [T89(97.9); S/T]	4350.7147	High	0.0002508	1.77E-07	3.5
FLDTNPIGAESFESSDGEMHLR	141-162	Ctp1	241	(no modification)	2452.10853	High	0.000211	1.99E-14	6.6
			1	1xPhospho [S155(99.3)]	2532.07486	High	0.000211	2.72E-05	4.64
			8	2xPhospho [S154(100); S155(100)]	2612.04119	High	0.000211	0.004061	2.25
		Ctp1p (5min)	142	(no modification)	2452.10853	High	0.0002365	8.37E-13	6.55
			56	1xPhospho [S155(99.6)]	2532.07486	High	0.0002365	2.82E-07	5.43
			52	2xPhospho [S154(100); S155(100)]	2612.04119	High	0.0002365	4.16E-05	4.08
		Ctp1p (full)	64	(no modification)	2452.10853	High	0.0002508	2.01E-15	6.84
			30	1xPhospho [S155(99.4)]	2532.07486	High	0.0002508	1.54E-07	5.46
			144	2xPhospho [S154(100); S155(100)]	2612.04119	High	0.0002508	3.07E-06	5.1
			19	3xPhospho [S151(100); S154(100); S155(100)]	2692.00752	High	0.0002508	7.63E-06	2.4

Table S2. Strains used in this study

Strain name	Related Genotype	Plasmid	Source or reference
YA119	*h⁻ Msmt-0 ura4-D18 leu1-32 his3-D1 arg3-D1*		Akamatsu et al., 2008
YST046	*Same as YA119 but ctp1::ura4⁺*		Akamatsu et al., 2008
YA1097	*h⁺ his3-D1 leu1-32 ura4-D18 ade6-M210 ctp1::ura4⁺*		Akamatsu et al., 2008
spAZ_063	Same as YST046	pREP81-Ctp1	This study
spAZ_064	Same as YST046	pREP81	This study
spAZ_090	Same as YST046	pREP81-Ctp1(F287A)	This study
spAZ_091	Same as YST046	pREP81-Ctp1(E289A)	This study
spAZ_092	Same as YST046	pREP81-Ctp1(F292A)	This study
spAZ_093	Same as YST046	pREP81-Ctp1(P284A)	This study
spAZ_094	Same as YST046	pREP81-Ctp1(P280A)	This study
spAZ_095	Same as YST046	pREP81-Ctp1(FWE-5A)	This study
spAZ_096	Same as YST046	pREP81-Ctp1(FWE-3A)	This study
spAZ_099	Same as YST046	pREP81-Ctp1(W288A)	This study
spAZ_114	Same as YA119 but *ctp1-F287A-KanMx6⁺*		This study
spAZ_120	Same as YA119 but *ctp1-W288A-KanMx6⁺*		This study
spAZ_123	Same as YA119 but *ctp1-F292A-KanMx6⁺*		This study
spAZ_128	Same as YA119 but *ctp1-(1-286)-KanMx6⁺*		This study

spAZ_132	Same as YA119 but *ctp1-(1-279)-KanMx6*$^{+}$		This study
spAZ_134	Same as YA119 but *ctp1-KanMx6*$^{+}$		This study
spAZ_156	Same as YA119 but *ctp1::KanMx6*$^{+}$		This study
spAZ_178	Same as YST046	pREP81-Ctp1(H274A, R275A)	This study
spAZ_184	Same as YST046	pREP81-Ctp1(C226S, C229S)	This study
spAZ_191	Same as YA119 but *ctp1-(H274A, R275A)-KanMx6*$^{+}$		This study
spAZ_196	Same as YA119 but *ctp1-(C226S, C229S)-KanMx6*$^{+}$		This study

Table S3. Primers used in this study

Designation	Sequence
oAZ_087	CAAAAAGTAGGCCGGGCTGCAAAATTAAACATCCCCAAAC
oAZ_088	GTTTGGGGATGTTTAATTTTGCAGCCCGGCCTACTTTTTG
oAZ_094	TCTCAATTCATGGTAATTCCGATGACCCTTCTGGT
oAZ_095	ACCAGAAGGGTCATCGGAATTACCATGAATTGAGA
oAZ_153	TGGAGCCACCCGCAGTTC
oAZ_158	GAACTGCGGGTGGCTCCAGTCATTCCAAGTAGGCGCAACG
oAZ_203	AGGTAAATCGCGCATTCTGTTCCCGGGCACCTATATCGTTGGTCGAAATGTATCT GACGATTCGTCCCACATTC
oAZ_204	GGATCCTTACTTATCGTCGTCATCCTTGTAATCAAAGTG
oAZ_205	GACGATAAGTAAGGATCCGAATTCGAGCTCCGTC
oAZ_206	AGAATGCGCGATTTACCTTTCAGGATATCGCCTTCCGCTTCAATAATCCACATATG TATATCTCCTTCTTAAAGTTAAACAAAATTATTTCTAGAG
oAZ_235	GAAAGCCCGGATAGCCAAAAGTTCTATGAGTTACATGGTCCAGTCAAAG
oAZ_236	TTGGCTATCCGGGCTTTCGTAAGCAGGAAGTGCTTTACGTTTATTAC
oAZ_265	CTGGAAGTTCTGTTCCAGGGGCCCGGTGGTAGCGGTGGTAGCCATCATCATCAT CATCACTGATAAGGATCCGAATTCGAGCTCCGTC
oAZ_266	CTGGAACAGAACTTCCAGCTTATCGTCGTCATCCTTGTAATCAAAGTGAAAC
oAZ_458	TCACATATGTCTGACAACCGCCAGAAAAAG
oAZ_514	GCTTACGAATCTCCGGATTCTCAAAAGGTAAGAGTATTTTTGGCTTTTTTCCCTAC
oAZ_515	TACCTTTTGAGAATCCGGAGATTCGTAAGCAGGAAGTGCTTTACGTTTATTACC
oAZ_516	TAGGCCGGGCTGCTAAATTAAACATCCCCAAACCTATTCCAAATGG
oAZ_517	TGGGGATGTTTAATTTAGCAGCCCGGCCTACTTTTTGCACCAAAGG
oAZ_522	GCTTACGAATCTCCGGATTCTCAAAAGTTCTATGAGTTACATGGTCCAGTCAA
oAZ_523	GAACTTTTGAGAATCCGGAGATTCGTAAGCAGGAAGTGCTTTACGT
PSOL10009	GAATTGTTAATTAAGTCAGTGATGATGATGATGATGATCATCTAAAATTTCGTCATCC

PSOL10010	TTGAAAATTCGAATTAAAAAAATGTCGTGCATTGACAGAATGTCCATCATG
PSOL10011	GAATTGTTAATTAAGTTAAAGAGGTTCTTTAACAATCATGCTCTTCTGATTCGTGTC
PSOL9975	TTATCCACTTCCAATGTTATTATCACTTATCGTCGTCATCCTTGTAATCAAAGTGAA ACTTGAGATCATTAAATTCATCG
T7ter	GCTAGTTATTGCTCAGCGG

SI References

1. S. L. Forsburg, N. Rhind, Basic methods for fission yeast. *Yeast* **23**, 173–183 (2006).
2. J. A. Young, R. W. Hyppa, G. R. Smith, Conserved and nonconserved proteins for meiotic DNA breakage and repair in yeasts. *Genetics* **167**, 593–605 (2004).
3. Y. Akamatsu, *et al.*, Molecular Characterization of the Role of the Schizosaccharomyces pombe nip1+/ctp1+ Gene in DNA Double-Strand Break Repair in Association with the Mre11-Rad50-Nbs1 Complex. *Mol. Cell. Biol.* **28**, 3639–3651 (2008).
4. M. Ueno, *et al.*, Molecular Characterization of the Schizosaccharomyces pombe nbs1+ Gene Involved in DNA Repair and Telomere Maintenance. *Mol. Cell. Biol.* **23**, 6553–6563 (2003).
5. R. E. Johnson, L. Prakash, S. Prakash, "Yeast and Human Translesion DNA Synthesis Polymerases: Expression, Purification, and Biochemical Characterization" in *Methods in Enzymologyethods Enzymol*, (2006), pp. 390–407.
6. F. W. Studier, Protein production by auto-induction in high density shaking cultures. *Protein Expr. Purif.* **41**, 207–234 (2005).
7. S. Sugita, *et al.*, Electrostatic interactions between middle domain motif-1 and the AAA1 module of the bacterial ClpB chaperone are essential for protein disaggregation. *J. Biol. Chem.* **293**, 19228–19239 (2018).
8. C. Pinto, R. Anand, P. Cejka, "Methods to Study DNA End Resection II: Biochemical Reconstitution Assays" in *Methods in Enzymology*, (2018), pp. 67–106.